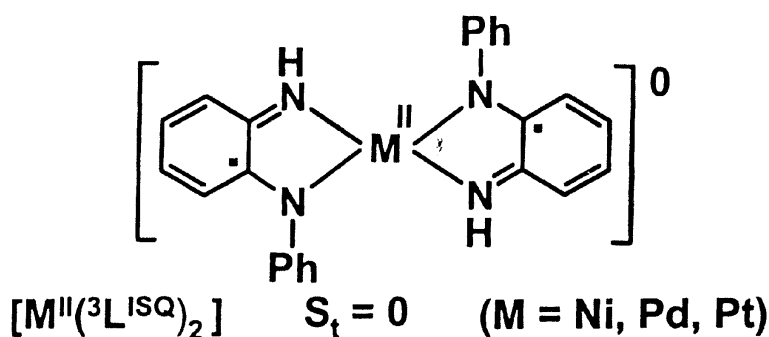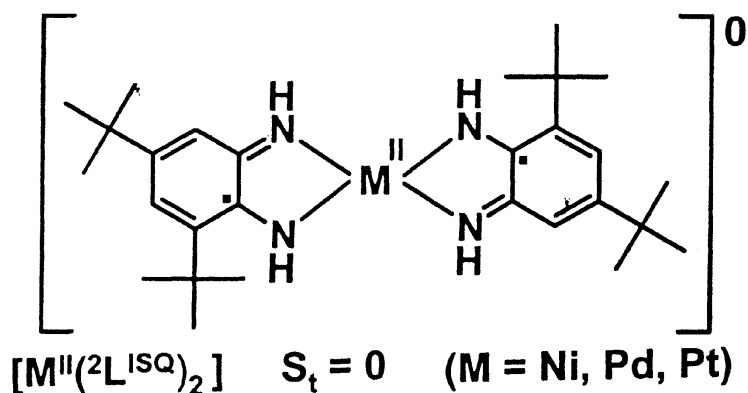## Article

Molecular and Electronic Structures of Bis-(*o*-diiminobenzosemiquinonato)metal(II) Complexes (Ni, Pd, Pt), Their Monocations and -Anions, and of Dimeric Dications Containing Weak Metal–Metal Bonds

Diran Herebian, Eberhard Bothe, Frank Neese, Thomas Weyhermller, and Karl Wieghardt

$[M^{II}(^{2}L^{ISQ})_2]$ $S_t = 0$ (M = Ni, Pd, Pt)

$[M^{II}(^{3}L^{ISQ})_2]$ $S_t = 0$ (M = Ni, Pd, Pt)

More About This Article

Additional resources and features associated with this article are available within the HTML version:

- Supporting Information
- Links to the 26 articles that cite this article, as of the time of this article download

- Access to high resolution figures
- Links to articles and content related to this article
- Copyright permission to reproduce figures and/or text from this article

View the Full Text HTML

Molecular and Electronic Structures of Bis-(*o*-diiminobenzosemiquinonato)metal(II) Complexes (Ni, Pd, Pt), Their Monocations and -Anions, and of Dimeric Dications Containing Weak Metal−Metal Bonds

Diran Herebian, Eberhard Bothe, Frank Neese, Thomas Weyhermüller, and Karl Wieghardt*

Contribution from the Max-Planck-Institut für Strahlenchemie, Stiftstrasse 34−36, D-45470 Mülheim an der Ruhr, Germany

Received February 19, 2003; E-mail: wieghardt@mpi-muelheim.mpg.de

Abstract: Two series of square planar, diamagnetic, neutral complexes of nickel(II), palladium(II), and platinum(II) containing two *N,N*-coordinated *o*-diiminobenzosemiquinonate(1-) π radical ligands have been synthesized and characterized by UV−vis and ^{1}H NMR spectroscopy: $[M^{II}(^2L^{ISQ})_2]$, M = Ni (**1**), Pd (**2**), Pt (**3**), and $[M^{II}(^3L^{ISQ})_2]$ M = Ni (**4**), Pd (**5**), Pt (**6**). $H_2[^2L^{PDI}]$ represents 3,5-di-*tert*-butyl-*o*-phenylenediamine and $H_2[^3L^{PDI}]$ is *N*-phenyl-*o*-phenylenediamine; $(L^{ISQ})^{1-}$ is the *o*-diiminobenzosemiquinonate π radical anion, and $(L^{IBQ})^0$ is the *o*-diiminobenzoquinone form of these ligands. The structures of complexes **1**, **4**, **5**, and **6** have been (re)determined by X-ray crystallography at 100 K. Cyclic voltammetry established that the complete electron-transfer series consisting of a dianion, monoanion, neutral complex, a mono- and a dication exists: $[M(L)_2]^z$ $z = -2, -1, 0, 1+, 2+$. Each species has been electrochemically generated in solution and their X-band EPR and UV−vis spectra have been recorded. The oxidations and reductions are invariably ligand centered. Two o-diiminobenzoquinones(0) and two fully reduced o-diiminocatecholate-(2-) ligands are present in the dication and dianion, respectively, whereas the monocations and monoanions are delocalized mixed valent class III species $[M^{II}(L^{ISQ})(L^{IBQ})]^+$ and $[M^{II}(L^{ISQ})(L^{PDI})]^-$, respectively. One-electron oxidations of **1** and trans-**6** yield the diamagnetic dications $\{cis\text{-}[Ni^{II}(^2L^{ISQ})(^2L^{IBQ})]_2\}Cl_2$ (**7**) and $\{trans\text{-}[Pt^{II}(^3L^{ISQ})(^3L^{IBQ})]_2\}(CF_3SO_3)_2$ (**8**), respectively, which have been characterized by X-ray crystallography; both complexes possess a weak M···M bond and the ligands adopt an eclipsed configuration due to weak bonding interactions via π stacking.

Introduction

In 1966, Balch and Holm[1] established that the reaction of *o*-phenylenediamine, $H_2(^1L^{PDI})$, with MX_2 salts (ratio 2:1) (M = Ni, Pd, Pt) affords in the presence of air dark blue/black microcrystals of neutral, planar and diamagnetic complexes $[M(^1L^{ISQ})_2]$ (Scheme 1) where $(L^{ISQ})^{1-\bullet}$ represents the *o*-diiminobenzosemiquinonate oxidation level. They have also shown that an electron-transfer series of five bis(chelate)metal

$[M^{II}(^1L^{ISQ})_2]$ $S_t = 0$ (M = Ni, Pd, Pt)
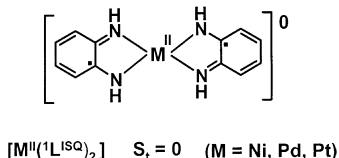
complexes of the general type $[M-N_4]^z$ with $z = -2, -1, 0, +1, +2$ exists where the species are interrelated by four reversible one-electron-transfer steps.

The nature of these redox steps as ligand- or metal-centered processes has been a matter of considerable debate. As early as
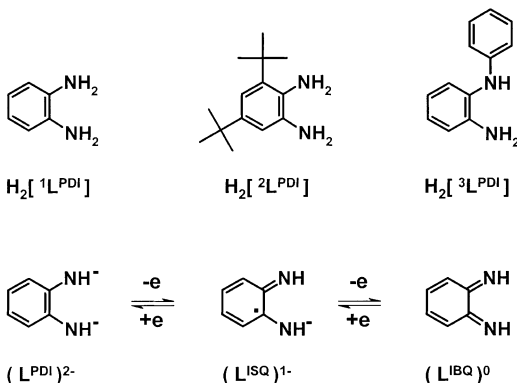
1965, Stiefel, Waters, Billig, and Gray[2] refuted the idea of the occurrence of Ni(I), Ni(III), or Ni(IV) in this series and proposed that all redox processes are ligand-centered and that the spectroscopic oxidation state of the central nickel ion is +II (d^8) throughout the above series of five complexes. The same holds true for the Pd and Pt species of the series.

(1) Balch, A. L.; Holm, R. H. *J. Am. Chem. Soc.* **1966**, *88*, 5201.

(2) Stiefel, E. I.; Waters, J. H.; Billig, E.; Gray, H. B. *J. Am. Chem. Soc.* **1965**, *87*, 3016.

(3) Swartz Hall, G.; Soderberg, R. H. *Inorg. Chem.* **1968**, *7*, 2300.

(4) (a) Cheng, H.-Y.; Lin, C.-C.; Tzeng, B.-C.; Peng, S.-M. *J. Chin. Chem. Soc.* **1994**, *41*, 775. (b) Sidorov, A. A.; Danilov, P. V.; Nefedov, S. E.; Golubnichaya, M. A.; Fomina, I. G.; Ellert, O. G.; Novotortsev, V. M.; Eremenko, I. L. *Russ. J. Inorg. Chem.* **1998**, *43*, 846; translated from *Zh. Neorg. Khim.* **1998**, *43*, 930.

(5) (a) Eremenko, I. L.; Nefedov, S. E.; Sidorov, A. A.; Pomina, M. O.; Danilov, P. V.; Stromnova, T. A.; Stolarov, I. P.; Katser, S. B.; Orlova, S. T.; Vargaftik, M. N.; Moiseev, I. I.; Ustynyuk, Yu. A. *J. Organomet. Chem.* **1998**, *551*, 171. (b) Reshetnikov, A. V.; Sidorov, A. A.; Talismanov, S. S.; Aleksandrov, G. G.; Ustynyuk, Yu. A.; Nefedov, S. E.; Eremenko, I. L.; Moiseev, I. I. *Russ. Chem. Bull., Int. Ed.* **2000**, *49*, 1771.

(6) Fomina, I. G.; Talismanov, S. S.; Sidorov, A. A.; Ustynyuk, Yu. A.; Nefedov, S. E.; Eremenko, I. L.; Moiseev, I. I. *Izv. Akad. Nauk. Ser. Khim.* **2001**, *50*, 499; translated in English: *Russ. Chem. Bull., Int. Ed.* **2001**, *50*, 515.

(7) Reshetnikov, A. V.; Talismanova, M. O.; Sidorov, A. A.; Nefedov, S. E.; Eremenko, I. L.; Moiseev, I. I. *Russ. Chem. Bull., Int. Ed.* **2001**, *50*, 142.

(8) (a) Peng, S.-M.; Chen, C.-T.; Liaw, D.-S.; Chen, C.-I.; Wang, Y. *Inorg. Chim. Acta* **1985**, *101*, L31. (b) Cheng, P.-H.; Cheng, H.-Y.; Lin, C.-C.; Peng, S.-M. *Inorg. Chim. Acta* **1990**, *169*, 19. (c) Nèmeth, S.; Simandi, L. I.; Argay, G.; Kálman, A. *Inorg. Chim. Acta* **1989**, *166*, 31.
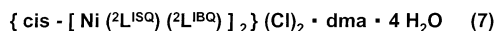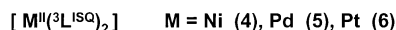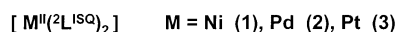
Scheme 1. Ligands and Complexes

Ligands and Abbreviations

$H_2[\ ^1L^{PDI}]$ $H_2[\ ^2L^{PDI}]$ $H_2[\ ^3L^{PDI}]$

$(\ ^{}L^{PDI})^{2-}$ $(\ L^{ISQ})^{1-}$ $(\ L^{IBQ})^0$

Complexes

$[\ M^{II}(^2L^{ISQ})_2]$ M = Ni (1), Pd (2), Pt (3)

$[\ M^{II}(^3L^{ISQ})_2]$ M = Ni (4), Pd (5), Pt (6)

$\{\ cis - [\ Ni\ (^2L^{ISQ})\ (^2L^{IBQ})\ ]\ _2\ \}\ (Cl)_2 \cdot dma \cdot 4\ H_2O$ (7)

$\{\ trans - [\ Pt\ (^3L^{ISQ})\ (^3L^{IBQ})\ ]\ _2\ \}\ (CF_3SO_3)_2$ (8)

In this early discussion the EPR spectra of the paramagnetic monocations ($S = \frac{1}{2}$) and of the paramagnetic monoanions ($S = \frac{1}{2}$) of this series played an important role and some interesting features remained poorly understood. For example, the EPR spectrum of the monocation $[Ni^{II}(^1L^{ISQ})(^1L^{IBQ})]^+$ exhibits a signal at $g \approx 2$ with a rather small, unresolved g-anisotropy ($g = 1.997$) whereas the corresponding monoanion $[Ni^{II}(^1L^{ISQ})(^1L^{PDI})]^-$ displays a signal with significant g-anisotropy ($g_1 = 1.990$, $g_2 = 2.006$, $g_3 = 2.102$).[1] In the early 1970s, no consensus model had been developed for this observation.

The neutral, diamagnetic complexes are structurally ill defined. Due to crystallographic problems the early X-ray structure determination of $[Ni^{II}(^1L^{ISQ})_2]$ is of rather poor quality[3] and does not allow a meaningful discussion of the structural features of the *N,N*-coordinated ($^1L^{ISQ})^{1-}$ ligands (Scheme 1). Three other room temperature crystal structure determinations of such neutral, square planar complexes, namely $[Ni^{II}(^3L^{ISQ})_2]$,[4] $[Pt(^3L^{ISQ})_2]$,[5] and $[Pt(C_6H_4(NH)(NCH_3))_2]$,[6] have been reported but these are also of rather low quality.

The situation is confusing because even the composition of the species of the series $[M(^3L^{ISQ})_2]$ (M = Ni, Pd, Pt) is incorrectly given in ref 4b, and 5 but correctly in the earlier(!) ref 4a. The authors[4b,5] have incorrectly formulated the *N,N*-coordinated ligands as deprotonated *o*-diiminebenzo-quinone(1-), namely $(^3L^{IBQ}\text{-}H)^{1-}$.

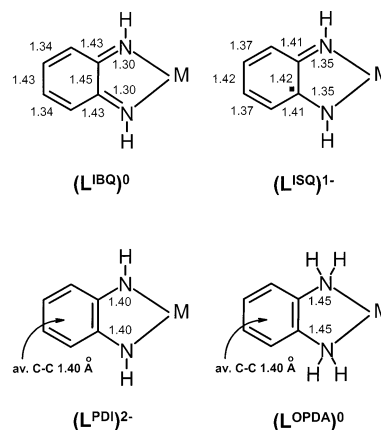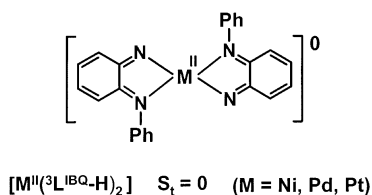$[M^{II}(^3L^{IBQ}\text{-}H)_2]$ $S_t = 0$ (M = Ni, Pd, Pt)

Figure 1. Average bond distances (Å) in *N,N*-coordinated ligands $(L^{IBQ})^0$, $(L^{ISQ})^{1-\bullet}$, $(L^{PDI})^{2-}$, and $(L^{OPDA})^0$ as determined by X-ray crystallography.

These species would contain 2 hydrogen atoms less than the correct formulation as $[M(^3L^{ISQ})_2]$. We will show here by mass spectrometry and X-ray structure determinations at 100 K that the latter is correct.[4a,7]

The most accurate structure determination of a planar complex containing two *N,N*-coordinated *o*-diiminobenzosemiquinonato-(1-) π radicals has been reported by Peng et al. for $[Co^{II}(^1L^{ISQ})_2]$[8a] and for five-coordinate, square base pyramidal $[Co^{III}(^1L^{ISQ})_2(py)]Cl$[8b] (py = pyridine) and, similarly, $[Co^{III}(^1L^{ISQ})_2(PPh_3)](ClO_4)$.[8c] The geometrical details[9] of the ligand are summarized in Figure 1. From the crystal structures of low spin $[Fe^{II}(^1L^{IBQ})_3](PF_6)_2$,[8] $[Fe^{II}(CN)_4(^1L^{IBQ})]^{2-}$,[10] $[Os^{II}(^1L^{IBQ})_3](ClO_4)_2$,[11] and $[Cu^I(N-Ch\text{-}bqdi)_2]Cl$[12] (N-Ch-bqdi = *N*-cyclohexyl-*o*-benzoquinonediimine) the bond distances of *N,N*-coordinated, neutral *o*-diiminobenzoquinone ligands, $(L^{IBQ})^0$, are established, and, similarly, from structure determinations of $[(n\text{-}Bu)_4N][TcO(^1L^{PDI})_2]$[13] and $[Mo(^1L^{PDI})(CO)_2(PPh_3)_2]$[14] those of *N,N*-coordinated, aromatic *o*-diiminophenolato(2-) ligands, $(^1L^{PDI})^{2-}$. Finally, *N,N*-coordinated *o*-phenylenediamine, $(L^{OPDA})^0$, complexes have also been characterized by X-ray crystallography; the data are also given in Figure 1; they are taken from ref 15 for $[Ni(OPDA)_4]Cl_2 \cdot 2OPDA$. From these previous studies,[9] it is therefore clear that both the level of protonation and oxidation of *N,N*-coordinated *o*-phenylene-diamine derived ligands can be established from high-quality, low-temperature X-ray crystallography.

The electronic structure of these neutral, planar, diamagnetic molecules has been studied by theoretical calculations[16,17] but only recently have DFT calculations[18] shown that $[Ni(^1L^{ISQ})_2]$ is best described as diradical with a singlet ground state as was

(9) (a) Mederos, A.; Dominguez, S.; Hernandez-Molina, R.; Sanchiz, J.; Brito, F. *Coord. Chem. Rev.* **1999**, *193–195*, 913. (b) Carugo, O.; Djinovic, K.; Rizzi, M.; Castellani, C. B. *J. Chem. Soc., Dalton Trans.* **1991**, 1551.
(10) Christoph, G. C.; Goedken, V. L. *J. Am. Chem. Soc.* **1973**, *95*, 3869.
(11) Ghosh, A. K.; Peng, S.-M.; Paul, R. L.; Ward, M. D.; Goswami, S. *J. Chem. Soc., Dalton Trans.* **2001**, 336.
(12) Cheng, H.-Y.; Tzeng, B.-C.; Peng, S.-M. *Bull. Inst. Chem., Acad. Sci.* **1994**, *41*, 51.
(13) Gerber, T. I. A.; Kemp, H. J.; du Preez, J. G. H.; Bandoli, G.; Dolmella, A. *Inorg. Chim. Acta* **1992**, *202*, 191.
(14) Anillo, A.; Obeso-Rosete, R.; Lanfranchi, M.; Tiripicchio, A. *J. Organomet. Chem.* **1993**, *453*, 71.
(15) Elder, R. C.; Koran, D.; Mark, H. B., Jr. *Inorg. Chem.* **1974**, *13*, 1644.
(16) Weber, J.; Daul, C.; von Zelewsky, A.; Goursot, A.; Penigault, E. *Chem. Phys. Lett.* **1982**, *88*, 78.
(17) Lelj, F.; Rosa, A.; Riccardi, G. P.; Casarin, M.; Cristinziano, P. L.; Morelli, G. *Chem. Phys. Lett.* **1989**, *160*, 39.
(18) Bachler, V.; Olbrich, G.; Neese, F.; Wieghardt, K. *Inorg. Chem.* **2002**, *41*, 4179.

suggested by Gray et al.[2] in 1965. Thus, two *N,N*-coordinated *o*-diiminobenzosemiquinonate(1-) π radicals couple intramolecularly, strongly antiferromagnetically yielding the observed $S = 0$ ground state and a quinoid type distorted ligand geometry. A singlet−triplet energy gap of ∼3000 cm^{-1} has been calculated.[18]

The electronic structures of the corresponding, paramagnetic monocations $[M^{II}(L^{ISQ})(L^{IBQ})]^+$ and monoanions $[M^{II}(L^{ISQ})(L^{PDI})]^-$ are much less well characterized. A first attempt has been made recently[19] where the monocation $[Pt^{II}(L_0^{ISQ})(L_0^{IBQ})]^+$ and the anion $[Pt^{II}(L_0^{ISQ})(L_0^{PDI})]^-$ have been characterized by DFT calculations (L_0 = *N*-phenyl-*o*-aminophenol derivatives).

The present work has been initiated to gain more insight into the electronic structures of these cations and anions and to resolve some puzzling experimental data. For instance, solutions of such monocations have repeatedly been reported to be EPR silent. On the other hand, solid, paramagnetic $[Ni^{II}({}^1L^{ISQ})({}^1L^{IBQ})]I$ has been described[1] and its EPR spectrum has been reported. We show here that these monocations can dimerize in solution yielding diamagnetic dimers $[M^{II}(L^{ISQ})(L^{IBQ})]_2^{2+}$ with a weak M···M (M = Ni, Pt) bond. Complexes of this type containing unsaturated tetraamine macrocycles have been reported but the nature of the Ni···Ni bond has not been explained satisfactorily.[20,21] The same group of refs 5 and 22 has reported two crystal structures of dimeric complexes allegedly containing Pt(III) with again *N,N*-coordinated, monodeprotonated monoanions of neutral ($^1L^{IBQ}$) and ($^3L^{IBQ}$); namely $\{[Pt^{III}({}^1L^{IBQ}\text{-}H)_2]_2\}(CF_3SO_3)_2$ and $\{cis\text{-}[Pt^{III}({}^3L^{IBQ}\text{-}H)_2]_2\}(CF_3SO_3)_2$. We will show here that each of these dications contains in fact four additional protons and must be formulated as $\{[Pt^{II}({}^1L^{ISQ})({}^1L^{IBQ})]_2\}(CF_3SO_3)_2$ and $\{cis\text{-}[Pt^{II}({}^3L^{ISQ})({}^3L^{IBQ})]_2\}(CF_3SO_3)_2$, respectively.

To avoid crystallographic problems of the kind encountered previously[3] for $[Ni^{II}({}^1L^{ISQ})_2]$ where severe stacking in the solid state gives rise to static disorder problems, we employed two bulkier ligands, namely 3,5-di-*tert*-butyl-*o*-phenylenediamine, $H_2[^2L^{PDI}]$, and N-phenyl-*o*-phenylenediamine, $H_2[^3L^{PDI}]$, (Scheme 1) and investigated the spectro- and electrochemistry of the neutral complexes $[M(^2L^{ISQ})_2]$ (M = Ni (**1**), Pd (**2**), Pt (**3**)) and $[M(^3L^{ISQ})_2]$ (M = Ni (**4**), Pd (**5**), and Pt (**6**)).

$[M^{II}(^2L^{ISQ})_2]$ $S_t = 0$ (M = Ni, Pd, Pt)
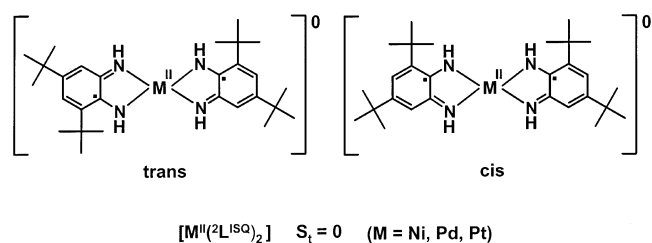
The correct[4a] and a flawed[4b] crystal structures of **4** (both determined at 25 °C) have been reported as have those of **5** and **6** (flawed).[5] Correct crystal structures of **4**·C$_6$H$_6$ and **6**·C$_6$H$_6$ determined at 22 °C have recently been reported.[5b] Here

we report a redetermination of these structures at 100 K.

$[M^{II}(^3L^{ISQ})_2]$ $S_t = 0$ (M = Ni, Pd, Pt)
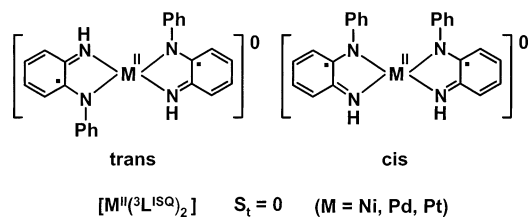
Recently, we have characterized the *N,N*-coordinated π radical anion, $(^3L^{ISQ})^{1-\bullet}$, in crystals of $[Pd^{II}(bpy)(^3L^{ISQ})]PF_6$ by X-ray crystallography.[23]

From oxidation reactions of **1** (with air) and *trans*-**6** with Ag$^+$ ions the diamagnetic complexes $\{cis\text{-}[Ni^{II}(^2L^{ISQ})(^2L^{IBQ})]_2\}Cl_2$ (**7**) and $\{trans\text{-}[Pt^{II}(^3L^{ISQ})(^3L^{IBQ})]_2\}(CF_3SO_3)_2$ (**8**) have been isolated and structurally characterized. Both complexes contain a weak M···M interaction at 2.800(1) and 3.197(1) Å, respectively.

Experimental Section

Preparation of Complexes. The ligand 3,5-di-*tert*-butyl-*o*-phenylenediamine, $H_2[^2L^{PDI}]$, was prepared according to published procedures.[24] *N*-Phenyl-*o*-phenylenediamine, $H_2[^3L^{PDI}]$, was commercially available (Sigma-Aldrich).

***trans/cis*-[Ni^{II}(^{2}L^{ISQ})$_2$] (1).** To a solution of the ligand H_2-[$^2L^{PDI}$]·2HCl (292 mg; 1.0 mmol) in a water/ethanol mixture (1:1% Vol; 30 mL) was added NiCl$_2$·6H$_2$O (120 mg; 0.5 mmol) and aqueous NH$_3$ (25%, 2 mL). The mixture was heated at 70 °C in the presence of air for 3 h. A dark blue microcrystalline precipitate formed which was collected by filtration, washed with cold water and dried in vacuo. Yield: 210 mg (85%). Single crystals of *trans*-**1** suitable for X-ray crystallography were obtained from a CH$_2$Cl$_2$/*n*-hexane mixture (1:1) by slow evaporation of the solvent in a stream of argon. EI-MS: *m/z* calcd for C$_{28}$H$_{44}$N$_4$Ni: 495.4; found 494. Anal. Calcd: C, 67.89; H, 8.95; N, 11.31; Found: C, 67.9; H, 9.1; N, 11.2. ^{1}H NMR (CD$_2$Cl$_2$, 500 MHz, 300 K): δ = 1.27 (s, 9H), 1.55 (s, 9H), 6.82 (d, 2H), 7.24 (br, 1NH), 7.44 (br, 1NH). ^{13}C NMR (CD$_2$-Cl$_2$, 125 MHz, 300 K): δ = 30.6, 31.0, 35.0, 35.1, 112.9, 118.7, 138.3, 146.4, 152.0, 157.5.

***trans-/cis*-[Pd(^{2}L^{ISQ})$_2$] (2).** To a solution of $H_2[^2L^{PDI}]$·2HCl (292 mg; 1.0 mmol) in a water/acetonitrile mixture (1:1% Vol; 30 mL) was added PdCl$_2$ (88 mg; 0.5 mmol) and aqueous NH$_3$ (25%, 2 mL). The mixture was heated at 70 °C in the presence of air for 2 h. A dark black precipitate formed which was collected by filtration, washed with cold water and dried in vacuo. Yield: 184 mg (68%). EI−MS: *m/z* Calcd for C$_{28}$H$_{44}$N$_4$-Pd: 543.1; found 542. Anal. Calcd: C, 61.92; H, 8.17; N, 10.32; Found: C, 61.7; H, 7.9; N, 10.2. ^{1}H NMR (CD$_2$Cl$_2$, 400 MHz, 300 K): δ = 1.27 (s, 18H), 1.53 (s, 18H), 6.69 (d, 2H), 6.73 (br, 2H), 7.42 (br, 2H), 7.66 (br, 2NH). ^{13}C NMR (CD$_2$Cl$_2$, 100 MHz, 300 K): δ = 30.6, 31.0, 34.9, 35.0, 113.4, 119.4, 137.8, 147.0, 154.1, 159.3.

***trans-/cis*-[Pt(^{2}L^{ISQ})$_2$] (3).** The complex was prepared as described above for **2** by using PtCl$_2$ (133 mg; 0.5 mmol) as starting material. Yield: 186 mg (59%). EI−MS: *m/z* calcd for

(19) Sun, X.; Chun, H.; Hildenbrand, K.; Bothe, E.; Weyhermüller, T.; Neese, F.; Wieghardt, K. *Inorg. Chem.* **2002**, *41*, 4296.
(20) (a) Millar, M.; Holm, R. H. *J. Am. Chem. Soc.* **1975**, *97*, 6052. (b) Peng, S.-M.; Ibers, J. A.; Millar, M.; Holm, R. H. *J. Am. Chem. Soc.* **1976**, *98*, 8037.
(21) Peng, S.-M.; Goedken, V. L. *J. Am. Chem. Soc.* **1976**, *98*, 8500.
(22) Sidorov, A. A.; Pomina, M. O.; Nefedov, S. E.; Eremenko, I. L.; Ustynyuk, Yu. A.; Luzikov, Yu. M. *Zh. Neorg. Khim.* **1997**, *42*, 952; translated to English: *Russ. J. Inorg. Chem.* **1997**, *42*, 853.

(23) Ghosh, P.; Begum, A.; Herebian, D.; Bothe, E.; Hildenbrand, K.; Weyhermüller, T.; Wieghardt, K. *Angew. Chem., Int. Ed. Engl.* **2003**, *42*, 563.
(24) (a) Burgers, J.; van Hartingsveldt, W.; van Keulen, J.; Verkade, P. E.; Visser, H.; Wepster, B. M. *Recueil* **1956**, *75*, 1327. (b) Stegmann, H. B.; Hieke, K.; Ulmschneider, K. B.; Scheffler, K. *Chem. Ber.* **1976**, *109*, 2243.

$C_{28}H_{44}N_4Pt$: 631.8; found 631. Anal. Calcd: C, 53.23; H, 7.02; N, 8.87; Found: C, 53.1; H, 7.1; N, 8.9. ^1H NMR (CD_2Cl_2, 400 MHz, 300 K): $\delta = 1.25/1.31$ (s, 9H), 1.41/1.48 (s, 9H), 6.82/6.66 (d, 2H), 8.49/8.65/6.90 (br, 2NH). ^{13}C NMR (CD_2Cl_2, 100 MHz, 300 K): $\delta = 30.2, 30.7, 31.6, 31.7, 34.4, 34.7, 35.1, 35.7, 112.9, 113.1, 115.3, 115.8, 126.3, 134.5, 135.3, 139.8, 141.7, 147.8, 152.4, 154.2$ (*cis* and *trans*-isomer ratio ~1:1).

trans-[Ni^II(^3L^ISQ)_2] (4). To a solution of the ligand $H_2[^3L^{PDI}]$ (368 mg; 2 mmol) in pyridine (10 mL) was added Ni(ClO_4)_2· 6H_2O (366 mg; 1 mmol) and NEt_3 (1 mL). The mixture was heated at 50 °C in the presence of air for 3 h. After filtration, the filtrate was kept for 1–2 d at −20 °C. A dark blue-black microcrystalline precipitate formed which was collected by filtration. Yield: 215 mg (51%). Single crystals suitable for X-ray crystallography were obtained from a CH_2Cl_2 solution by slow evaporation of the solvent. EI−MS: *m/z* calcd for $C_{24}H_{20}N_4Ni$: 423.2; found 422. Anal. Calcd: C, 68.13; H, 4.76; N, 13.24; Found: C, 68.2; H, 4.7; N, 13.2. ^1H NMR (CD_2Cl_2, 400 MHz, 300 K): $\delta = 6.09$ (br, 1NH), 6.66 (m, 4H), 7.49 (ddd, 1H), 7.55 (ddd, 2H), 7.62 (ddd 2H). ^{13}C NMR (CD_2Cl_2, 100 MHz, 300 K): $\delta = 116.6, 119.0, 123.5, 123.9, 126.5, 128.6, 128.7, 149.9, 154.8, 155.3$.

trans-[Pd^II(^3L^ISQ)_2] (5). To a solution of the ligand $H_2[^3L^{PDI}]$ (368 mg; 2 mmol) in water/acetonitrile (1:1, 20 mL) was added PdCl_2 (177 mg; 1 mmol) and NEt_3 (1 mL). The solution was stirred under reflux for 3 h in the presence of air. After storing the solution for 1 d at room temperature, a dark blue-green crystalline precipitate formed. Recrystallization of the compound from CH_2Cl_2/-hexane (1:1) at 4 °C gave dark blue crystals suitable for X-ray diffraction. The yield was 250 mg (53%). EI−MS: *m/z* calcd for $C_{24}H_{20}N_4Pd$: 470.8; found 470. Anal. Calcd: C, 61.22; H, 4.28; N, 11.90; Found: C, 61.2; H, 4.2; N, 11.8. ^1H NMR (CD_2Cl_2, 400 MHz, 300 K): $\delta = 6.07$ (s, br, 1NH), 6.55 (m, 1H), 6.64 (ddd, 2H), 6.75 (d, 1H), 7.35 (ddd 1H), 7.44 (dd, 2H), 7.51 (ddd, 2H). ^{13}C NMR (CD_2Cl_2, 100 MHz, 300 K): $\delta = 116.4, 119.7, 123.9, 124.7, 126.1, 127.2, 128.9, 149.3, 155.6, 158.0$.

trans-[Pt^II(^3L^ISQ)_2](trans-6) and cis-[Pt^II(^3L^ISQ)_2] (cis-6). To a solution of the ligand $H_2[^3L^{PDI}]$ (368 mg; 2 mmol) in water/acetonitrile (1:1, 20 mL) was added PtCl_2 (266 mg; 1 mmol) and NEt_3 (1 mL). The mixture was heated at 70 °C in the presence of air for 3 h. The dark blue reaction mixture was left for 1 day at room temperature. A microcrystalline precipitate was collected by filtration and washed twice with 5 mL of cold water. As judged from the ^1H NMR spectrum, this crude material is a 1:1 mixture of the trans- and cis-isomers. The product was separated into the trans- and cis-isomers by HPLC on a Nucleosil-7-C18 column (Abimed Gilson 305 pump, 155 UV−vis detector operating at 280/700 nm), at 6 mL/min flow rate with MeOH as eluent. The first fraction contained the *trans*-isomer and the second one the *cis*-isomer. Black-blue prisms suitable for X-ray crystallography of the first fraction were grown from a CH_2Cl_2 solution at 4 °C. The overall yield of both isomers was ~66% (370 mg). EI−MS: *m/z* Calcd for $C_{24}H_{20}N_4Pt$: 559.5; Found 559 for *cis*- and *trans*-(**6**), respectively. Anal. Calcd: C, 51.52; H, 3.60; N, 10.01; found for *cis*-(**6**): C, 51.4; H, 3.7; N, 9.9 and *trans*-(**6**): C, 51.5; H, 3.5; N, 10.0. ^1H NMR of *cis*-(**6**) (CD_2Cl_2, 400 MHz, 300 K): $\delta = 6.24$ (d, 1H), 6.47 (dd, 1H), 6.72 (dd, 1H), 6.82 (dd, 2H), 6.98 (dd,

2H), 7.05 (m, 2H), 8.58 (br, 1NH). *trans*-(**6**): $\delta = 6.61$ (ddd, 1H), 6.71 (ddd, 1H), 6.86 (dd, 2H), 7.25 (br, 1NH), 7.46 (m, 1H), 7.62 (dd, 4H). ^{13}C NMR (CD_2Cl_2, 100 MHz, 300 K): *cis*-(**6**): $\delta = 117.1, 118.3, 123.0, 124.1, 126.1, 127.8, 129.1, 148.3, 154.1, 156.4$. *trans*-(**6**): $\delta = 116.0, 119.4, 123.5, 123.9, 126.9, 127.8, 129.1, 149.1, 154.7, 156.0$

{cis-[Ni^II(^2L^ISQ)(^2L^IBQ)]_2}Cl_2 (7). To a solution of the ligand $H_2[^2L^{PDI}]·2HCl$ (292 mg; 1.0 mmol) in methanol (40 mL) was added NiCl_2·6H_2O (120 mg; 0.5 mmol) and NEt_3 (2 mL). The mixture was stirred at room temperature in the presence of air for 24 h. A dark red-black microcrystalline precipitate formed which was collected by filtration, washed with cold methanol and dried in vacuo. Yield: 150 mg (28%). Single-crystals of **7**(dma)·4H_2O suitable for X-ray crystallography were obtained from a *N,N*-dimethylacetamide (dma) solution by slow evaporation of the solvent. ESI-MS (pos. ion, CH_2Cl_2): *m/z* Calcd for $\{7-Cl\}^+$ 1026.2; Found 1025. Anal. Calcd for $C_{56}H_{88}N_8Cl_2Ni_2$: C, 63.36; H, 8.35; N, 10.55; Found: C, 63.2; H, 8.4, N, 10.4. ^1H NMR (CD_2Cl_2, 400 MHz, 300 K): $\delta = 1.12$ (s, 18H), 1.48 (s, 18H), 6.05 (d, 2H), 6.82 (d, 2H), 9.25 (br, 2NH), 9.85 (br, 2NH). ^{13}C NMR (CD_2Cl_2, 125 MHz, 300 K): $\delta = 30.3, 30.9, 35.1, 35.5, 117.2, 126.5, 141.1, 152.8, 157.5, 159.9$.

{trans-[Pt^II(^3L^ISQ)(^3L^IBQ)]_2}(CF_3SO_3)_2 (8). To a solution of trans-**6** (0.10 g; 0.18 mmol) in acetone (15 mL) was added Ag^I-triflate (46 mg; 0.18 mmol). The mixture was stirred at room temperature for 1 h and then filtered. The solvent was stripped off by rotary evaporation and the solid residue was extracted with CH_2Cl_2 (40 mL). The volume of the brown solution was reduced to ~15 mL by evaporation. The resulting solution was stored at 4 °C for 1 d after which time a brown crystalline precipitate had formed in 70% yield (89 mg). X-ray quality crystals were grown from a CH_2Cl_2/benzene (5:1 Vol) solution topped with a layer of pentane. Anal. Calcd for $C_{50}H_{40}F_6N_8O_6Pt_2S_2$: C, 42.38; H, 2.84; N, 7.91; Found: C, 42.3; H, 2.9; N, 7.8. ^1H NMR (CD_2Cl_2, 400 MHz, 300 K): $\delta = 6.20–7.52$ (br, 9H), 8.71 (1 NH), 9.38 (1NH).

Physical Measurements. Electronic spectra of complexes and spectra of the spectroelectrochemical measurements were recorded with a Perkin-Elmer Lambda 9 spectrophotometer (range: 200−2000 nm). Cyclic and square-wave voltammograms and coulometric experiments were performed with an EG&G potentiostat/galvanostat. X-band EPR spectra were recorded with a Bruker ESP 300 spectrometer.

X-ray Crystallographic Data Collection and Refinement of the Structures. Dark green single crystals of **4**, **5**, and **6**, a black crystal of **1** and **8**, respectively, and a dark violet crystal of **7** were coated with perfluoropolyether, picked up with a glass fibers and mounted in the nitrogen cold stream of the diffractometers. Intensity data were collected at 100 K using graphite monochromated Mo−Kα radiation ($\lambda = 0.71073$ Å). Final cell constants were obtained from a least-squares fit of a subset of several thousand strong reflections. Data collection was performed by hemisphere runs taking frames at 1.0° in ω, except for **6** where a scan width of 0.3° was used. Crystal faces of **1**, **4**, **5**, **6**, and **8** were determined and the Gaussian type empirical absorption correction embedded in XPREP[27] was used to correct

(25) Chaudhuri, P.; Verani, C. N.; Bill, E.; Bothe, E.; Weyhermüller, T.; Wieghardt, K. *J. Am. Chem. Soc.* **2001**, *123*, 2213.
(26) Herebian, D.; Bothe, E.; Bill, E.; Weyhermüller, T.; Wieghardt, K. *J. Am. Chem. Soc.* **2001**, *123*, 10 012.
(27) ShelXTL V.5, Siemens Analytical X-ray Instruments, Inc. 1994.

Table 1. Crystallographic Data for **1**, **4**, **5**, **6**, **7**·C$_4$H$_9$NO·4 H$_2$O, **8**

	1	4	5	6	7·C$_4$H$_9$NO·4 H$_2$O	8
chem. formula	C$_{28}$H$_{44}$N$_4$Ni	C$_{24}$H$_{20}$N$_4$Ni	C$_{24}$H$_{20}$N$_4$Pd	C$_{24}$H$_{20}$N$_4$Pt	C$_{60}$H$_{105}$Cl$_2$N$_9$O$_5$Ni$_2$	C$_{50}$H$_{40}$F$_6$N$_8$O$_6$Pt$_2$S$_2$
crystal size, mm^3	0.18 × 0.10 × 0.04	0.25 × 0.09 × 0.08	0.21 × 0.08 × 0.06	0.20 × 0.08 × 0.02	0.15 × 0.11 × 0.09	0.20 × 0.10 × 0.05
Fw	495.38	423.15	470.84	559.53	1220.85	1417.20
space group	$P2_1/c$, No. 14	$P\text{-}1$, No. 2	$P\text{-}1$, No. 2	$P\text{-}1$, No. 2	$P\text{-}1$, No. 2	$P2_1/n$, No. 14
a, Å	10.7105(12)	9.6222(6)	9.5312(6)	9.5122(9)	10.4103(9)	10.4524(4)
b, Å	9.5010(10)	10.2880(6)	10.2585(6)	10.2317(9)	10.4924(9)	15.1295(8)
c, Å	13.889(2)	11.5222(8)	11.7914(6)	11.793(10)	16.2202(12)	14.9194(8)
α, °	90	74.30(1)	73.74(1)	73.70(1)	104.21(2)	90
β, °	103.16(2)	75.88(1)	75.84(1)	75.82(1)	101.48(2)	98.982(6)
γ, °	90	62.74(1)	63.36(1)	63.35(1)	102.03(2)	90
V, Å	1376.2(3)	966.47(11)	979.73(10)	975.1(3)	1620.2(2)	2342.7(2)
Z	2	2	2	2	1	2
T, K	100(2)	100(2)	100(2)	100(2)	100(2)	100(2)
ρ calcd, g cm^{-3}	1.195	1.454	1.596	1.906	1.251	2.009
diffractometer used	Nonius Kappa-CCD	Nonius Kappa-CCD	Nonius Kappa-CCD	Siemens- SMART	Nonius Kappa-QCCD	Nonius Kappa-CCD
refl. collected/Θ_{max}	13274/60.00	11780/66.62	11863/66.30	7902/52.00	16191/60.00	25149/66.30
unique refl./$I > 2\sigma(I)$	3984/3206	7316/5626	7344/5509	3646/2125	9281/6861	8881/7450
no. params/restraints.	188/32	271/1	273/0	271/1	408/8	340/0
μ(Mo Kα), cm^{-1}	7.26	10.22	9.65	72.13	7.15	61.40
$R1^a$/goodness of fit^b	0.1058/1.210	0.0401/1.024	0.0331/ 1.009	0.0336/0.977	0.0634/1.040	0.0301/1.017
w$R2^c$ ($I > 2\sigma$ (I))	0.2363	0.0858	0.0714	0.0677	0.1467	0.0636

^{a} $I > 2\ \sigma(I)$. R1$=\sum||F_o| - |F_c||/\sum|F_o|$. ^{b} GooF$=[\sum[w(F_o{}^2 - F_c{}^2)^2]/(n - p)]^{1/2}$. ^{c} wR2 $= [\sum[w(F_o{}^2 - F_c{}^2)^2]/\sum[w(F_o{}^2)^2]]^{1/2}$ where $w = 1/\sigma^2(F_o{}^2)+(aP)^2 + bP$, $P = (F_o{}^2 + 2F_c{}^2)/3$.

for absorption. Intensity data of **7** were corrected using the semiempirical correction routine MulScanAbs.[28] The ShelXTL[27] software package was used for solution, refinement and artwork of the structure which was readily solved by Patterson methods and difference Fourier techniques. All non-hydrogen atoms were refined anisotropically and hydrogen atoms bound to carbon were placed at calculated positions and refined as riding atoms with isotropic displacement parameters. Hydrogen atoms bonded to the coordinating nitrogen atoms were located from the difference map and were isotropically refined with restrained N−H bond distances using the SADI instruction in ShelX97. A disordered *tert*-butyl group in **1** (C(11)−C(14)) was split on two positions with equal occupation factors keeping the C−C distances restrained to be equal within a certain error. Disorder also occurred in the structure of **7**, where the chloride anion, a water molecule, and a dimethylacetamide solvent molecule were split on two positions to account for this problem. Crystallographic data of the compounds and diffractometer types used are listed in Table 1. Further information on structure refinement can be found in the Supporting Information.

Results

Syntheses of Complexes. The reaction of the bis(hydrochloride) of 3,5-di-*tert*-butyl-*o*-phenylenediamine, H$_2$(^{2}L^{PDI}), in an ethanol/water mixture (1:1 Vol) with 0.5 equiv of NiCl$_2$·6H$_2$O at 70 °C in the presence of air and aqueous ammonia as base afforded a blue-black microcrystalline precipitate in 85% yield. Recrystallization of this material from a CH$_2$Cl$_2$/*n*-hexane mixture (1:1 Vol) gave single crystals of *trans*-[Ni^{II}(^{2}L^{ISQ})$_2$] (**1**). The corresponding blue-black complexes of a mixture of *cis*- and *trans*-isomers of [Pd(^{2}L^{ISQ})$_2$] (**2**) and [Pt^{II}(^{2}L^{ISQ})$_2$] (**3**) were prepared analogously. The ^{1}H NMR spectrum of a CD$_2$Cl$_2$ solution of the crude product of **3** exhibits two sets of proton signals at a ratio of ∼1:1 corresponding to the *cis*- and *trans*-isomers of **3**. Similar solutions of **1** and **2** display only one set of signals which split into two sets upon lowering the temper-

(28) PLATON program suite by Spek, A. L., University of Utrecht, The Netherlands, 1999.

ature. Thus, the *cis*- and *trans*-forms of **1** and **2** are in a rapid equilibrium at 25 °C. Similar behavior has been reported for [M(L$_s^{ISQ}$)$_2$] where (L$_s^{ISQ}$)$^{1-}$ represents the radical anion of 2,4-di-*tert*-butyl-6-aminothiophenol, H[L$_s^{AP}$].[26]

These measurements prove **1**, **2**, and **3** to be diamagnetic at 25 °C ($S = 0$).

We have not been able to separate the *cis*-/*trans*-isomers of **1**, **2**, and **3** using high-pressure-liquid chromatography (HPLC). The EI mass spectra of **1**, **2**, and **3** each display a molecular ion peak {M}$^+$ which clearly indicates the presence of four N-bonded protons per metal ion. The isotopic pattern of the {M}$^+$ peak is in all cases in excellent agreement with a composition C$_{28}$H$_{44}$N$_4$M (M = Ni, Pd, Pt).

In the infrared spectrum each species displays two sharp ν(N−H) stretching frequencies at 3357, 3412 cm^{-1} for **1**, 3328, 3425 cm^{-1} for **2**, and 3346, 3423 cm^{-1} for **3**. This is in accord with the fact that the two imine groups in the two *N,N*-coordinated ligands (^{2}L^{ISQ})$^{1-}$ are chemically not equivalent (see below). For [Ni^{II}(4-i-pr-C$_6$H$_3$(NH)$_2$)$_2$] also two ν(N−H) bands at 3367, 3475 cm^{-1} have been reported.[1]

Similarly, the reaction of *N*-phenyl-*o*-phenylenediamine, H$_2$-(^{3}L^{PDI}), with an MCl$_2$ or M(ClO$_4$)$_2$·nH$_2$O salt (M = Ni, Pd, Pt) in pyridine or a water/acetonitrile mixture containing an equivalent of triethylamine as base at 70 °C in the presence of air yields blue-black microcrystalline solids [M^{II}(^{3}L^{ISQ})$_2$] (M = Ni (**4**), Pd (**5**), Pt (**6**)). The single crystals obtained after slow recrystallization of **4** and **5** contain exclusively the respective *trans*-isomer.

The crude material of **6** was found to be a mixture of the *cis*- and *trans*-isomers as was judged from the ^{1}H NMR spectrum. By using HPLC separation on a Nuclesil-7-C18 column and CH$_3$OH as eluent, it has been possible to isolate pure solid samples of *trans*-**6** (1st fraction) and *cis*-**6** (2nd fraction).

The infrared spectra of *trans*-**4**, *trans*-**5**, and *trans*-**6** each display two closely related, sharp ν(N−H) stretching frequencies at 3343, 3354 cm^{-1} for **4**, at 3339, 3351 cm^{-1} for **5**, and at 3346, 3358 cm^{-1} for *trans*-**6**. This is in excellent agreement

with their crystal structure determinations where it is shown that two crystallographically independent, *N,N*-coordinated ($^3L^{ISQ}$)$^{1-}$ ligands are present in the unit cell. The EI mass spectra of **4**, **5**, and **6** display a molecular ion peak {$C_{24}H_{20}N_4M$}$^+$ with the correct isotope pattern (M = Ni, Pd, Pt), respectively. The compounds are diamagnetic ($S = 0$).

Thus, the present crystallographic (see below) and spectroscopic data are compatible only with a formulation as [M^{II}($^3L^{ISQ}$)$_2$] as reported by Cheng et al.[4a] for **4** and not as [M($^3L^{IBQ}$-H)$_2$] as reported by Sidorov et al.[4b,5] for **4**, **5**, and **6**. We note that the latter authors recently changed[7] their original incorrect formulation of **4** and **6**[5b] to the correct one without providing an explanation or new data.

We have discovered that air oxidation of a mixture of the ligand H$_2$[$^2L^{PDI}$]·2HCl and NiCl$_2$·6H$_2$O in CH$_3$OH in the presence of the base triethylamine yields a diamagnetic microcrystalline solid product of {*cis*-[Ni^{II}($^2L^{ISQ}$)($^2L^{IBQ}$)]$_2$}Cl$_2$ (**7**). Recrystallization of this material from *N,N*-dimethylacetamide (dma) yielded single crystals of **7**·(dma)·4H$_2$O suitable for X-ray crystallography (see below). Interestingly, the ^{1}H NMR spectrum of **7** in CD$_2$Cl$_2$ solution (see the Experimental Section) differs significantly from that of neutral **1**. It proves that **7** is diamagnetic even in solution and, most importantly, that all four organic ligands are equivalent on the time scale of an ^{1}H NMR experiment ($\sim$10^{-7} s). In agreement with this interpretation solutions of **7** are EPR silent.

Interestingly, the oxidation reaction of [Pt^{II}($^1L^{ISQ}$)$_2$] with Ag$^+$ ions yields a diamagnetic dimer which the original authors[22] have characterized by X-ray crystallography and described it as Pt(III) species {[Pt^{III}($^1L^{IBQ}$-H)$_2$]$_2$}(CF$_3$SO$_3$)$_2$. Similarly,[5] when they oxidized crude [Pt^{II}($^3L^{ISQ}$)$_2$] with Ag$^+$ they obtained a diamagnetic dimer which they described as {*cis*-[Pt^{III}($^3L^{IBQ}$-H)$_2$]$_2$}(CF$_3$SO$_3$)$_2$. We have oxidized *trans*-**6** with one equivalent of Ag(CF$_3$SO$_3$) in acetone and obtained a diamagnetic brown precipitate of {*trans*-[Pt^{II}($^3L^{ISQ}$)($^3L^{IBQ}$)]$_2$}(CF$_3$SO$_3$)$_2$. We show here that the description of the two complexes is only compatible with the reported structural details[5,22] as {[Pt^{II}($^1L^{ISQ}$)($^1L^{IBQ}$)]$_2$}(CF$_3$SO$_3$)$_2$ and {*cis*-[Pt^{II}($^3L^{ISQ}$)($^3L^{IBQ}$)]$_2$}(CF$_3$SO$_3$)$_2$. Thus, both compounds contain four N-bonded protons per dimeric dication more than the authors in ref 5 and 20 have indicated.

Crystal Structures. The crystal structures of complexes **1**, **4**, **5**, **6**, **7** (dma)·4H$_2$O, and **8** have been determined by X-ray crystallography at 100(2) K. Table 1 gives crystallographic data and Table 2 summarizes important bond lengths. Figure 2 displays the structure of a neutral molecule in crystals of **1**; Figure 3 shows a representative structure of **4** which is very similar to those of the neutral molecules in crystals of **5** and **6** (not shown); Figure 4 shows the dimer {[Ni($^2L^{ISQ}$)($^2L^{IBQ}$)]$_2$}$^{2+}$ in crystals of **7** and Figure 5 shows the dimeric dication in crystals of **8**.

The neutral molecule in crystals of **1** is planar; the central nickel(II) ion is *N,N*-coordinated to two *o*-diiminobenzosemiquinonate(1-) π radical anions as can be clearly seen from a comparison of the C−N and C−C bond lengths in **1** (Table 2) with those shown in Figure 1 for such coordinated radicals. The average C−N bond length at 1.352(5) Å and the quinoid type distortion of the six-membered ring with two alternating short C=C bonds at 1.382(6) Å and four longer C−C bonds at av. 1.426(6) Å is representative for an (L^{ISQ})$^{1-}$ radical anion.

Table 2. Selected Bond Distances (Å)

complex **1**			
Ni−N1	1.822(4)	C1−C6	1.429(6)
Ni−N2	1.826(4)	C1−C2	1.435(6)
N1−C1	1.356(5)	C2−C3	1.386(6)
N2−C6	1.347(5)	C3−C4	1.423(6)
C5−C6	1.415(6)	C4−C5	1.379(6)

complex **4, 5, 6**			
	4 (M1=Ni)	**5** (M1=Pd)	**6** (M1=Pt)
M1−N1	1.823(1)	1.961(2)	1.933(8)
M1−N2	1.861(1)	1.985(2)	1.977(8)
M2−N3	1.822(1)	1.961(2)	1.952(7)
M2−N4	1.863(1)	1.985(2)	1.980(7)
N1−C1	1.340(2)	1.338(3)	1.364(11)
N2−C2	1.358(2)	1.357(3)	1.367(12)
N2−C7	1.426(2)	1.426(3)	1.444(11)
C1−C6	1.416(2)	1.422(3)	1.400(11)
C1−C2	1.435(2)	1.441(3)	1.423(12)
C2−C3	1.413(2)	1.421(3)	1.427(12)
C3−C4	1.378(2)	1.377(3)	1.375(11)
C4−C5	1.414(2)	1.414(3)	1.416(12)
C5−C6	1.373(2)	1.371(3)	1.346(12)
N3−C13	1.342(2)	1.341(2)	1.349(11)
N4−C14	1.358(2)	1.355(2)	1.341(12)
N4−C19	1.426(2)	1.428(2)	1.435(13)
C13−C18	1.413(2)	1.416(3)	1.418(11)
C13−C14	1.432(2)	1.443(3)	1.431(12)
C14−C15	1.413(2)	1.420(3)	1.442(12)
C15−C16	1.372(2)	1.371(3)	1.381(12)
C16−C17	1.416(2)	1.421(3)	1.410(13)
C17−C18	1.373(2)	1.369(3)	1.379(13)

complex **7, 8**			
	7	*a*	**8**
Ni···Ni	2.7996(9)	Pt···Pt	3.260(1)	3.1970(3)
Ni−N1	1.852(2)	Pt−N1	1.962(4)	1.975(2)
Ni−N6	1.831(2)	Pt−N2	2.019(5)	2.005(2)
Ni−N21	1.863(2)	Pt−N3	1.964(5)	1.966(2)
Ni−N26	1.827(2)	Pt−N4	2.024(4)	2.017(2)
N1−C1	1.320(3)	N1−C1	1.323(8)	1.329(3)
N6−C6	1.318(3)	N2−C2	1.322(7)	1.345(3)
N21−C21	1.321(3)	N2−C7	1.453(6)	1.434(4)
N26−C26	1.323(3)	N3−C21	1.321(8)	1.321(3)
		N4−C22	1.326(8)	1.348(3)
C1−C6	1.462(3)	N4−C27	1.456(6)	1.432(3)
C1−C2	1.455(3)	C1−C6	1.434(8)	1.427(4)
C2−C3	1.370(4)	C1−C2	1.459(7)	1.454(4)
C3−C4	1.448(3)	C2−C3	1.413(9)	1.424(4)
C4−C5	1.364(3)	C3−C4	1.334(9)	1.361(4)
C5−C6	1.431(3)	C4−C5	1.455(8	1.425(5)
		C5−C6	1.344(10)	1.361(4)
C21−C26	1.465(4)			
C21−C22	1.452(4)	C21−C26	1.419(9)	1.434(4)
C22−C23	1.367(4)	C21−C22	1.464(7)	1.457(4)
C23−C24	1.448(4)	C22−C23	1.429(9)	1.426(4)
C24−C25	1.368(4)	C23−C24	1.315(10)	1.363(4)
C25−C26	1.428(4)	C24−C25	1.439(8)	1.422(4)
		C25−C26	1.367(10)	1.356(4)

a Complex {*cis*-[Pt($^3L^{ISQ}$)($^3L^{IBQ}$)]$_2$}(CF$_3$SO$_3$)$_2$ from ref 5.

Interestingly, both imine protons have been located in the final difference Fourier map and were included in the refinement. Thus, in contrast to the earlier crystal structure determination of [Ni^{II}($^1L^{ISQ}$)$_2$] [3] it is possible for **1** to unambiguously assign spectroscopic oxidation states to the central nickel ion as +II (d^8) and the ligands as ($^2L^{ISQ}$)$^{1-}$ π radical anions. The structural features observed for **1** are fully in accord with DFT calculations on [Ni^{II}($^1L^{ISQ}$)$_2$].[18]

Similarly, the crystal structures of the neutral molecules in **4**, **5**, and **6** clearly show that both ligands are *N,N*-coordinated as π radical anions, ($^3L^{ISQ}$)$^{1-}$, rendering the oxidation state of the central metal ion +II (d^8). Note that the estimated standard
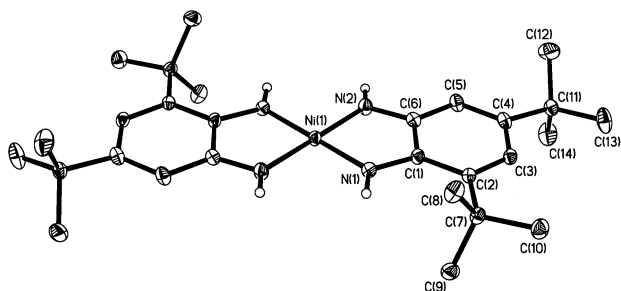
Figure 2. Structure of the neutral molecule in crystals of **1**. Small open circles represent imine hydrogen atoms; all other are omitted for the sake of clarity.
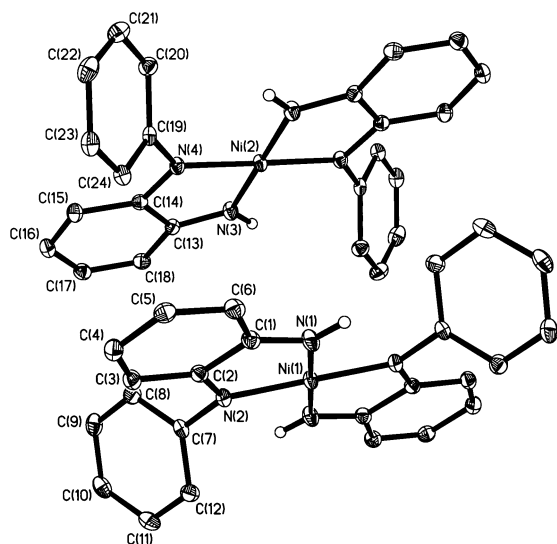

Figure 3. Structures of the two crystallographically independent molecules in crystals of **4**. Those of **5**, and **6** are very similar and not shown. The small open circles represent (located) imine hydrogen atoms; all other H atoms are not shown.
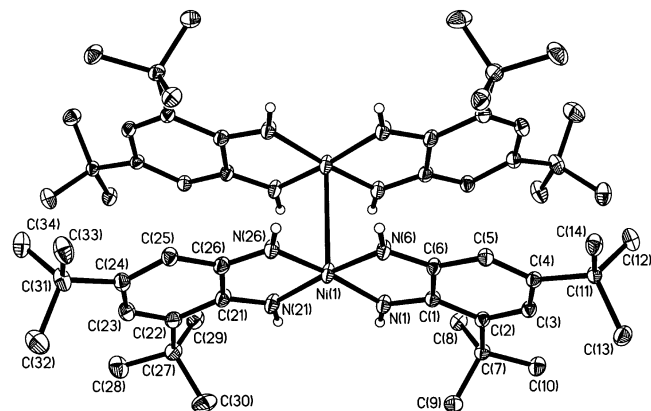

Figure 4. Structure of the dication {*cis*-[Ni^{II}(^{2}L^{ISQ})(^{2}L^{IBQ})]$_2$}$^{2+}$ in crystals of **7**. Small open circles represent (located) imine hydrogen atoms; all other H atoms are not shown. The chloride anion Cl1 forms hydrogen bonding contacts to the water molecule of crystallization (Cl1···O1 3.103 Å) and two *cis*-imine groups N1 and N21 (Cl1···N1 3.298 Å, Cl1···N21 3.293 Å). The water molecule of crystallization forms also two N−H···O hydrogen bonding contacts (O1···N6 2.958 Å, O1···N26 2.876 Å).

deviations in **4** and **5** are very small indeed. Therefore, the observed bond lengths are within ±0.009 Å (3σ) accurate. The same structural features of the ligands as described above for **1** are observed: short C−N bonds and quinoid type distorted six-membered rings. The N-phenyl groups serve as internal standards for the quality of the structure determinations because
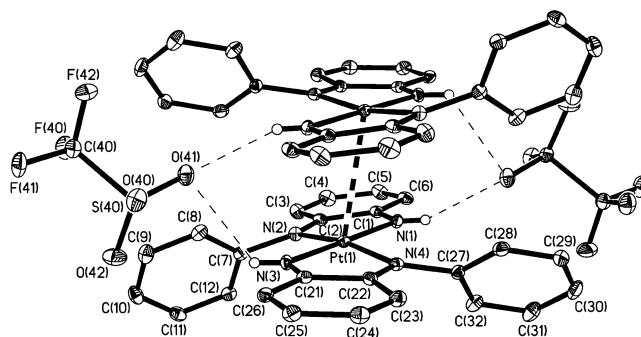
Figure 5. Structure of the dication {*trans*-[Pt(^{3}L^{ISQ})(^{3}L^{IBQ})]$_2$}$^{2+}$ in crystals of **8**. Small open circles represent (located) imine hydrogen atoms; all other H atoms are not shown.

the C−C distances are equidistant at 1.39 ±0.01 Å. The structure of **4** has been reported twice in the literature determined at ambient temperature in the correct space group $P\bar{1}$ ($Z = 2$)[4a,4b] but in ref 4b two imine protons have not been found. Similarly, in the structures of **5** and **6** the two imine protons have also not been found previously. The present structure determinations of **4**, **5**, and **6** unequivocally establish that each complex contains two *N,N*-coordinated *o*-diiminobenzosemiquinonate(1-) π radical anions and a central divalent metal ion: [M(^{3}L^{ISQ})$_2$] (M = Ni^{II}, Pd^{II}, Pt^{II}).

As shown in Figure 4, crystals of **7** contain a centrosymmetric dication where two *cis*-[Ni^{II}(^{2}L^{ISQ})(^{2}L^{IBQ})]$^+$ moieties are held together by a weak Ni···Ni interaction at 2.800(1) Å. The two halves of the dication adopt an eclipsed configuration and each half is not quite planar because the nickel ions are 0.141 Å above the plane defined by the four imine nitrogen atoms. This represents the most clear-cut structural evidence that a bonding Ni···Ni interaction is present. The imine protons at N1, N6, N21, and N26 have been located in the final difference Fourier map in excellent accord with the observation of two ν(N−H) stretching frequencies at 3354 and 3258 cm^{-1} in the infrared spectrum of **7**. Two *cis*-imine groups form two hydrogen bonding contacts to a chloride ion Cl···H−N at 3.298 and 3.293 Å which in turn is hydrogen bonded to a water molecule of crystallization Cl1···H−O1 (O1···Cl1 3.103 Å). The water molecule of crystallization is also hydrogen bonded to two *cis*-imine groups (N−H···O 2.958 and 2.876 Å). Note that the two *N,N*-coordinated ligands of each half of the dication adopt a *cis*-position relative to each other.

It is now of interest to compare the ligand dimensions in **7** with those of the neutral complex *trans*-[Ni^{II}(^{2}L^{ISQ})$_2$] **1**. The results of this comparison are schematically shown in Figure 6. Although the two ligands of one-half of the dimer in **7** are crystallographically independent, their metrical details (bond lengths and bond angles) are within ±0.012 Å (3σ) and ±0.6°, respectively, identical. Thus, the two ligands are equivalent on the time scale of X-ray crystallography at 100 K. An unsymmetrical, localized distribution of ligand oxidation levels as implied in the formulation [Ni^{II}(^{2}L^{ISQ})(^{2}L^{IBQ})]$^+$ appears to be ruled out by these results because deviations from a superposition of ligands of different structure would give average values, but with large esd's and distorted thermal ellipsoids. It is revealing that the average C−N distance at 1.352 ± 0.015 Å in **1** is significantly shorter at 1.320 ± 0.010 Å in **7**, where the estimated error represents 3σ. In the latter, the C−N distance represents the arithmetic average between the C−N bond lengths
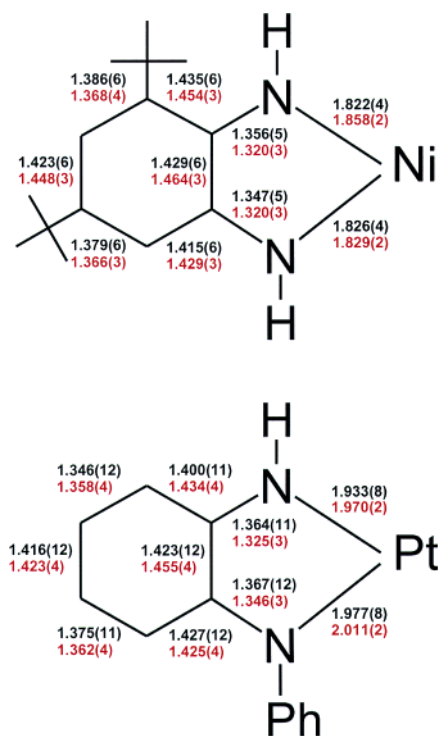
Figure 6. Comparison of the bond lengths within the *N,N*-coordinated ligands: Top: in neutral [Ni(^{2}L^{ISQ})$_2$] **1** and (in red) in {*cis*-[Ni(^{2}L^{ISQ})-(^{2}L^{IBQ})]$_2$}$^{2+}$ **7**; bottom: in **6** and (in red) in **8**.

in one (^{2}L^{ISQ})$^{1-}$ and a (^{2}L^{IBQ}) ligand (Figure 1). Thus, one electron oxidation of [Ni^{II}(^{2}L^{ISQ})$_2$] (**1**) is a ligand-centered process yielding a delocalized paramagnetic [Ni^{II}(L^{ISQ})(L^{IBQ})]$^+$ cation which dimerizes yielding a diamagnetic dication.

The structure of **8** comprising the dicationic, centrosymmetric dimer {*trans*-[Pt^{II}(^{3}L^{ISQ})(^{3}L^{IBQ})]$_2$}$^{2+}$ and two hydrogen bonded CF$_3$SO$_3$$^-$ anions is shown in Figure 5. The imine hydrogen atoms have again been located unequivocally in the final difference Fourier map which rules out its formulation as {[Pt^{III}(^{3}L^{IBQ}-H)$_2$]$_2$}$^{2+}$. As in **7**, the two crystallographically independent ligands of one-half-dimer are equivalent within the small 3σ limits. The av. C—N distance at 1.336 ± 0.01 Å is as in **7**; it is intermediate between those in (^{3}L^{ISQ})$^{1-}$ in **6** and (^{3}L^{IBQ}) in [Br$_2$Pt^{II}(^{3}L^{IBQ})].[5] In the infrared spectrum of **8** two ν(N—H) stretching frequencies are observed at 3440 and 3200 cm^{-1}; they are broadened due to hydrogen bonding to the CF$_3$SO$_3$$^-$ anions (N1···O41 2.933 Å, N3···O41 3.098 Å). The Pt···Pt interaction at 3.197(1) Å is weak. Note that the two *N,N*-coordinated ligands of each half of the dication adopt a *trans*-configuration relative to each other. Each half is not quite planar; the Pt^{II} ion is 0.085 Å above the plane defined by the four imine nitrogen atoms.

In the following we would like to comment on two recent crystal structure determinations[5,22] with striking similarity to that of **8**. Sidorov et al.[22] have reported the structure of a dinuclear complex which they have described as {[Pt^{III}(^{1}L^{IBQ}-H)$_2$]$_2$}-(CF$_3$SO$_3$)$_2$ where (^{1}L^{IBQ}-H)$^{1-}$ represents the mono-*N*-deprotonated, monoanionic form of *o*-diiminebenzoquinone, (^{1}L^{IBQ}). Thus, the chemical composition was assumed to be {[Pt(C$_6$H$_4$-(NH)(N))$_2$]$_2$}(CF$_3$SO$_3$)$_2$. Similarly, Eremenko et al.[5a] reported the structure of what they assumed to be {*cis*-[Pt^{III}(^{3}L^{IBQ}-H)$_2$]$_2$}-(CF$_3$SO$_3$)$_2$·2C$_6$H$_6$ where (^{3}L^{IBQ}-H)$^{1-}$ represents the mono-*N*-deprotonated, monoanionic form of *N*-phenyl-*o*-diiminobenzo-quinone, (^{3}L^{IBQ}). They assumed a chemical composition of
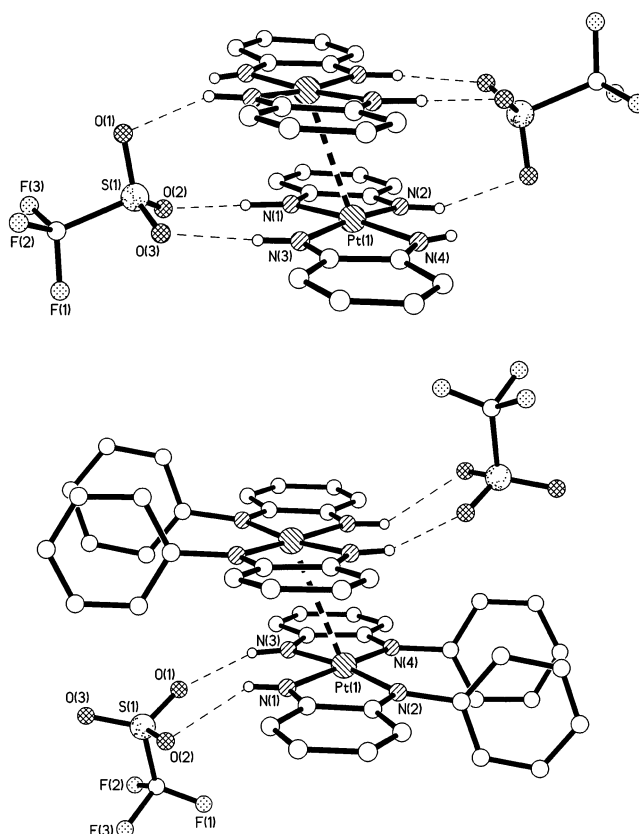

Figure 7. Structure of the dications in {[Pt(^{1}L^{ISQ})(^{1}L^{IBQ})]$_2$}(CF$_3$SO$_3$)$_2$ from ref 22 and {*cis*-[Pt(^{3}L^{ISQ})(^{3}L^{IBQ})]$_2$}(CF$_3$SO$_3$)$_2$·2C$_6$H$_6$ from ref 5. Atom coordinates were taken from the Cambridge Crystallographic Data Centre. The small open circles represent imine nitrogen atoms four of which had been neglected per dimer in ref 5, and 22, respectively. The positions of the protons at N1 and N3 of the former and at N2 and N3 of the latter structure have been calculated assuming sp^2 hybridized nitrogen atoms.

[C$_{48}$H$_{36}$N$_8$Pt$_2$](CF$_3$SO$_3$)$_2$·2C$_6$H$_6$. Figure 7 shows a schematic representation of both complexes.

It is interesting to note that the two ligands per half-dimer of the latter compound adopt a *cis*-configuration rather than *trans* as in **8**. The Pt···Pt distances are 3.031(4) Å in the former and 3.260(1) Å in the latter complex which compares well with that in **8** at 3.197 ± 0.001 Å. Interestingly, the C—N distances in both compounds and in **8** are also identical at ~1.32 Å as are the quinoid type distortions of the six-membered rings. Thus, we propose that both former complexes are in fact the two protons richer analogues of **8**, namely {[Pt^{II}(^{1}L^{ISQ})(^{1}L^{IBQ})]$_2$}-(CF$_3$SO$_3$)$_2$ and {*cis*-[Pt^{II}(^{3}L^{ISQ})(^{3}L^{IBQ})]$_2$}(CF$_3$SO$_3$)$_2$·2C$_6$H$_6$. Structural evidence for this notion may be taken from the original data.[5,22] The CF$_3$SO$_3$$^-$ anions in the former complex form O···H—N hydrogen bonds to the imine groups in {*cis*-[Pt(^{1}L^{ISQ})-(^{1}L^{IBQ})]$_2$}(CF$_3$SO$_3$)$_2$ as pointed out by the original authors:[22] N1···O2 2.98 Å. N2(N2a) and N3(N3a) are supposedly not protonated but the N2···O1 distance at 3.11 Å and that of N3···O2 at 2.94 Å indicate to us that both nitrogen atoms are actually protonated (see Figure 7). Thus, this complex contains four N-bonded protons more than suggested previously. The imine group at N4 is not involved in hydrogen bonding.

Similarly, it is possible to show that the nitrogen atoms N1 and N3 in {*cis*-[Pt^{II}(^{3}L^{ISQ})(^{3}L^{IBQ})]$_2$}(CF$_3$SO$_3$)$_2$·2C$_6$H$_6$ are both protonated and not deprotonated as suggested in ref 5. The CF$_3$SO$_3$$^-$ anions form again hydrogen bonding contacts to these
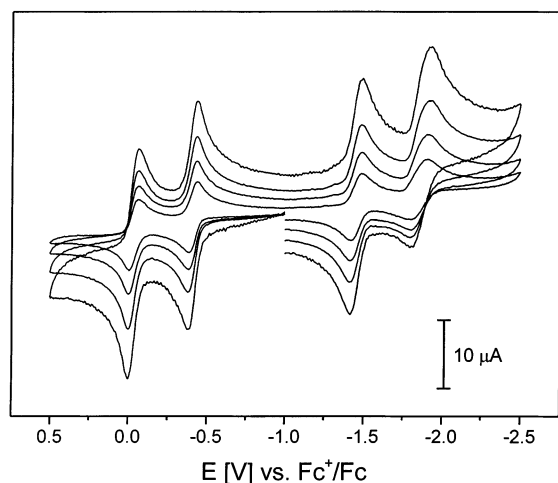
Figure 8. Representative cyclic voltammogram of **2** in acetonitrile solution (0.10 M [TBA]BF$_4$) at a glassy carbon working electrode and scan rates 50, 100, 200, 400 mV s^{-1}.

Table 3. Redox Potentials of Complexes at 20 °C^a in Volts vs Ferrocenium/Ferrocene (Fc$^+$/Fc)

complex	solvent	$E^1_{1/2}$, V	$E^2_{1/2}$, V	$E^3_{1/2}$, V	$E^4_{1/2}$, V
1	CH$_3$CN	−2.12	−1.46	−0.35	−0.15
	CH$_2$Cl$_2$	−2.17	−1.48	−0.56$_5$	+0.12
7	CH$_3$CN	−2.08	−1.46	−0.36	−0.17
2	CH$_3$CN	−1.86	−1.45	−0.41	−0.03
3	CH$_3$CN^b	−2.22	−1.57	−0.31	0.21
	c	−2.22	−1.84$_5$	0.03	0.21
4	CH$_2$Cl$_2$	−1.89	−1.21	−0.07	0.21
5	CH$_2$Cl$_2$	−1.72	−1.22	−0.14	0.24
6	CH$_2$Cl$_2$^{b}	−2.00	−1.37	−0.03	0.43
	c	−1.89	−1.38$_5$	−0.14	0.46

^{a} Scan rate 100 mV s^{-1}. ^{b} *trans*-form. ^{c} *cis*-form.

imine groups N1···O2 3.07 Å and N3···O1 2.85 Å as shown in Figure 7. In both structures, the Pt^{II} ions are located slightly above the N$_4$-planes, namely 0.089 Å in the former and 0.078 Å in the latter compound.

Spectro- and Electrochemistry. Cyclic voltammograms (cv) of all complexes have been recorded in CH$_2$Cl$_2$ or CH$_3$CN solutions containing 0.10 M [(*n*-Bu)$_4$N]PF$_6$ or [(*n*-Bu)$_4$N]BF$_4$ as supporting electrolyte at a glassy carbon working electrode and a Ag/AgNO$_3$ reference electrode. They are shown in Figure S1 (**1**, **3**) and S2 (**4**, **5**, **6**) and in Figure 8 for *trans*-**2**. Ferrocene (Fc) was used as an internal standard, and potentials are referenced versus the ferrocenium/ferrocene couple (Fc$^+$/Fc). Table 3 summarizes the results.

The cyclic voltammograms of **1**–**6** each display four reversible (in some cases quasi reversible) one-electron-transfer processes. The redox potentials for E$^1_{1/2}$ are observed in the narrow range −2.22 (−2.00) to −1.86 (−1.72), for complexes **1**–**3** and (in brackets) for **4**–**6**, those for E$^2_{1/2}$ in the range −1.57 (−1.385) to −1.46 (−1.22), those for E$^3_{1/2}$ in the range −0.31 (−0.14) to −0.56 (−0.07), and those for E$^4_{1/2}$ in the range 0.12 (0.46) to −0.17 (0.21) V irrespective of the nature of the central metal ion Ni, Pd, or Pt or the configuration of the ligands relative to each other (*cis* or *trans* as shown for **6**). Figure 8 shows a representative cv of *trans*-**2**. The insensitivity of the potentials is taken as evidence that these processes are all ligand-based (Scheme 2). We have found no evidence for a +I or +III oxidation state of the respective metal ion; they are all divalent metal ions in all neutral, cationic and anionic forms. The
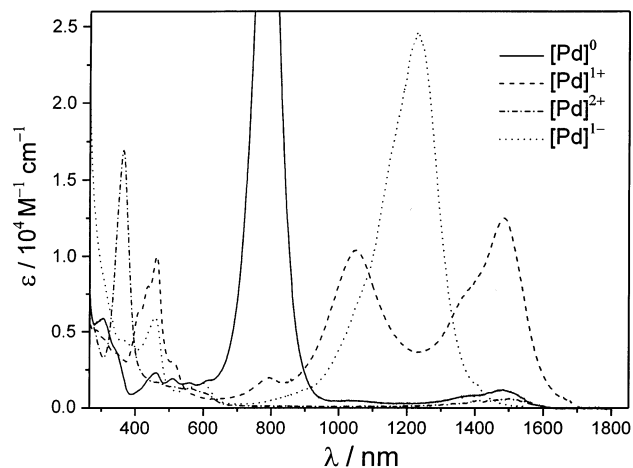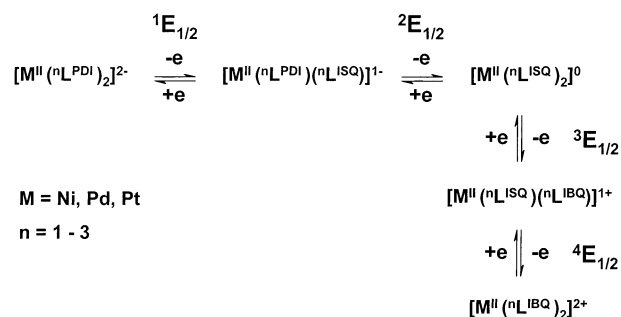
Figure 9. Spectra of **2** in acetonitrile solution (0.10 M [TBA]BF$_4$) and of electrochemically generated [**2**]$^+$, [**2**]$^{2+}$, [**2**]$^-$.

Scheme 2. Complete Electron Transfer Series of [M(^{n}L^{ISQ})$_2$] Complexes (n = 1−3, M = Ni, Pd, Pt)

$$^1E_{1/2} \qquad \qquad ^2E_{1/2}$$

$$[M^{II}(^nL^{PDI})_2]^{2-} \underset{+e}{\overset{-e}{\rightleftharpoons}} [M^{II}(^nL^{PDI})(^nL^{ISQ})]^{1-} \underset{+e}{\overset{-e}{\rightleftharpoons}} [M^{II}(^nL^{ISQ})_2]^0$$

M = Ni, Pd, Pt

n = 1 - 3

$$+e \| -e \quad ^3E_{1/2}$$

$$[M^{II}(^nL^{ISQ})(^nL^{IBQ})]^{1+}$$

$$+e \| -e \quad ^4E_{1/2}$$

$$[M^{II}(^nL^{IBQ})_2]^{2+}$$

electrochemistry resembles very much that of [M^{II}(^{1}L^{ISQ})$_2$] (M = Ni, Pd, Pt).[1]

Because the redox potentials are well separated from each other, we performed controlled potential electrolysis experiments to generate the oxidized mono- and dications of the neutral complexes as well as the reduced mono- and dianions in solution and recorded their electronic and X-band EPR spectra. Figure 9 shows a representative example and Table 4 summarizes the electronic spectra of complexes; Figures S3, S4, and S5 show the electronic spectra of all species, whereas Figures S6−S9 display the EPR spectra of the monocation and monoanions.

As has been pointed out for complexes of Ni^{II}, Pd^{II}, Pt^{II} containing two aminophenolate[25] or aminothiophenolate[26] ligands and their oxidized or reduced forms the electronic spectra of the neutral complexes, of the dications and dianions and of the monocations and monoanions are characteristic of the oxidation level of the two ligands irrespective of the nature of the central metal ion or the substitution pattern of the ligands. In line with this are the present observations for these five species: (i) The dications containing two neutral *o*-diiminobenzoquinone, (L^{IBQ})^0, ligands, [M^{II}(L^{IBQ})$_2$]$^{2+}$ display a very intense absorption maximum at 366−380 nm (1.0−1.8 × 10^4 M^{-1} cm^{-1}) and two weaker ones (∼0.4 × 10^4 M^{-1} cm^{-1}) at ∼480 and ∼580 nm. (ii) Similarly, the dianions [M^{II}(L^{PDI})$_2$]$^{2-}$ do not absorb at >400 nm (with intensity >500 M^{-1} cm^{-1}). (iii) The spectra of the monoanions are interesting because they all display a very intense (1.0−2.5 × 10^4 M^{-1} cm^{-1}) absorption in the near-infrared at 918 nm for [**3**]$^{1-}$ and 1316 nm for [**5**]$^{1-}$. This band is due to a mixed valent charge-transfer band of the [M^{II}(L^{PDI})(L^{ISQ})]$^{1-}$ species. In addition, a number of medium

Table 4. Electronic Spectra of Complexes

complex	solvent	λ_{max}, nm ($10^4 \epsilon$, M^{-1} cm^{-1})
[1]	CH₃CN	278sh(0.83), 334sh(0.36), 513sh(0.14), 621(0.41), 790(5.43)
[1]¹⁺ᵇ		296sh(0.50), 372(0.23), 521(0.90), 625(0.52), 792sh(0.47), 980(1.66), 1387(0.43)
[1]²⁺		319(0.41), 353sh(0.30), 373(0.32), 414(0.36)
[1]¹⁻		373sh(0.25), 457(0.67), 593(0.13), 791(0.25), 1031(1.95)
[4]	CH₂Cl₂	228(3.4), 278(0.2), 342sh(1.0), 411(0.2), 537sh(0.2), 629sh(0.4), 688sh(0.6), 839(4.0)
[4]¹⁺ᵇ		225(3.4), 311(1.2), 444(0.6), 640(0.7), 726sh(0.3), 1513(0.9)
[4]²⁺		428(0.7)
[4]¹⁻		227(4.0), 351sh(1.0), 459(0.6), 575sh(0.2), 623(0.4), 1119(1.7)
[4]²⁻		232(3.6), 279(2.4)
[2]	CH₃CN	305(0.60), 342sh(0.38), 462(0.23), 509(0.19), 558(0.16), 611(0.18), 788(4.40)
[2]¹⁺		289(0.51), 310(0.45), 348sh(0.38), 411sh(0.64), 437(0.81), 463(1.0), 512sh(0.3), 790(0.2), 1046(1.0), 1371sh(0.75), 1485(1.25)
[2]²⁺		380(1.7), 500(0.4)
[2]¹⁻		366sh(0.44), 460(0.60), 601(0.16), 1232(2.46)
[5]	CH₂Cl₂	252(2.6), 331(1.3), 417sh(0.2), 465(0.2), 544(0.2), 595sh(0.4), 650(0.4), 840(4.1)
[5]¹⁺		260(1.8), 340(0.8), 436sh(1.2), 461(1.5), 544sh(0.4), 1617(2.6)
[5]²⁺		261(1.4), 366(1.8), 579sh(0.4), 626sh(0.4)
[5]¹⁻		243(3.8), 364sh(1.0), 466(0.6), 585sh(0.2), 639(0.4), 1316(2.0)
trans-/cis-**[3]**	CH₃CN	366(0.52), 463(0.18), 556(0.24), 686sh(2.90), 715(5.82)
[3]¹⁺		294sh(0.93), 349sh(0.64), 368(0.76), 413sh(0.76), 439(0.93), 467sh(0.81), 544(0.47), 580(0.52), 869(0.93), 1082sh(0.35), 1165(0.41)
[3]²⁺		297sh(0.92), 362(1.40), 377(1.63), 446(0.64), 478(0.93), 528sh(0.41)
[3]¹⁻		367(0.58), 482(0.64), 531sh(0.17), 813sh(0.87), 918(1.39)
[6]	CH₂Cl₂	314(0.6), 378(0.2), 425sh(0.2), 479(0.2), 547sh(0.2), 589(0.4), 741(5.1)
[6]¹⁺ᵇ		305(0.4), 427(0.5), 466sh(0.5), 493(0.5), 548(0.6), 601(0.6), 746(1.0), 911(0.2), 1153sh(0.6), 1236(1.0)
[6]²⁺		224(2.8), 359sh(0.6), 377(0.9), 467(0.6), 545(0.4)
[6]¹⁻		225(2.2), 350sh(0.6), 481(0.3), 546sh(0.2), 753(0.4), 869sh(0.4), 982(0.7)

ᵃ The **[X]**¹⁺, **[X]**²⁺, **[X]**¹⁻, and **[X]**²⁻ species were generated electrochemically in the respective solvent con taining 0.10 M [(*n*-Bu)₄N]PF₆. ᵇ EPR silent solution; therefore, the spectrum may correspond to the respective dimeric diamagnetic dication or a mixture of mono- and dinuclear species: 2[**X**]¹⁺ ⇌ {[**X**]₂}²⁺. Absorption coefficients are always given per one metal ion.

Table 5. EPR Spectra of Electrochemically Generated Monocations and Monoanions of Complexes **1**−**6**

	g_x	g_y	g_z	g_{iso}	A_{xx}, G	A_{yy}, G	A_{zz}, G	ref
[1]⁺	silent							this work
[1]⁻	1.9938	2.0071	2.0991	2.0333				this work
[2]⁺	1.9995	1.9946	2.0022	1.9988				this work
[2]⁻	1.9533	2.0092	2.0616	2.0080				this work
[3]⁺	1.9645	2.0115	1.9865	1.9877	10.2	10.1	10.4	this work
[3]⁻ ᵃ⁾	2.0330	2.0214	1.9950	2.0165				this work
	2.0095	2.0095	1.9770	1.999				this work
[4]⁺	silent							this work
[4]⁻	1.9941	2.0066	2.0975	2.0327				this work
[5]⁺	1.9993	1.9995	2.0000	1.9996				this work
[5]⁻	1.9569	2.0103	2.0603	2.0092				this work
trans-**[6]**⁺	1.9635	1.9991	1.9960	1.9862	20	16	17	this work
trans-**[6]**⁻	1.8195	1.9860	2.2187	2.0081	14	178	126	this work
[Ni(¹Lᴵˢ۹)(¹Lᴵᴮ۹)]⁺						1.997	1	
[Ni(¹Lᴵˢ۹)(¹Lᴾᴰᴵ)]⁻		1.990		2.006	2.102	2.031	1	
[Pd(¹Lᴵˢ۹)(¹Lᴵᴮ۹)]⁺						1.997	1	
[Pd(¹Lᴵˢ۹)(¹Lᴾᴰᴵ)]⁻		1.946		2.008	2.062	2.006	1	
[Pt(¹Lᴵˢ۹)(¹Lᴵᴮ۹)]⁺						1.982	1	
[Pt(¹Lᴵˢ۹)(¹Lᴾᴰᴵ)]⁻		1.759		1.979	2.217	1.988	1	
[Niᴵᴵ(O,O)₂]⁻		1.998		2.015	2.121	2.045	29	
[Ni(O,S)₂]⁻		2.017		2.036	2.191	2.083	31	
[Ni(S,S)₂]⁻		2.016		2.048	2.183	2.082	30	
[Ni(N,S)₂]⁻		2.0056		2.0282	2.1147	2.067	26,31	

ᵃ Two signals of *cis*-**[3]**⁻ and *trans*-**[3]**⁻ in an approximately 1:1 ratio; it is not known which signal belongs to which isomer.

intense bands (∼0.2 × 10⁴ M^{-1} cm^{-1}) in the region 400−900 nm are characteristic of the presence of the radical anion (Lᴵˢ۹)¹⁻•. (iv) All neutral species [Mᴵᴵ(Lᴵˢ۹)₂] display a very intense band (ϵ (4.1−5.8) × 10⁴ M^{-1} cm^{-1}) in the region 715−840 nm. This band is a spin and dipole allowed ligand-to-ligand charge-transfer band. Medium intense bands in the region 400−800 nm are again indicative of the presence of radical anions (Lᴵˢ۹)¹⁻•. (v) Finally, because solutions containing the putative monocations, [Mᴵᴵ(Lᴵᴮ۹)(Lᴵˢ۹)]¹⁺, are EPR silent in the case of [**1**]¹⁺ and [**4**]¹⁺ we propose that the Ni-species have completely dimerized yielding the respective dinuclear, metal−metal bonded

dication. For the other cases which do show EPR spectra (Table 5), it is not established what the magnitude of the equilibrium constant K in eq 1 actually is

$$2\,[M^{II}(L^{ISQ})(L^{IBQ})]^+ \overset{K}{\rightleftharpoons} \{[M^{II}(L^{ISQ})(L^{IBQ})]_2\}^{2+} \quad (1)$$

Because the electronic spectra are governed by the presence of the mixed valence CT band of one (Lᴵˢ۹)¹⁻ radical anion and an *o*-diiminobenzoquinone ligand, Lᴵᴮ۹, the spectra of the mononuclear paramagnetic monocation and of the dinuclear
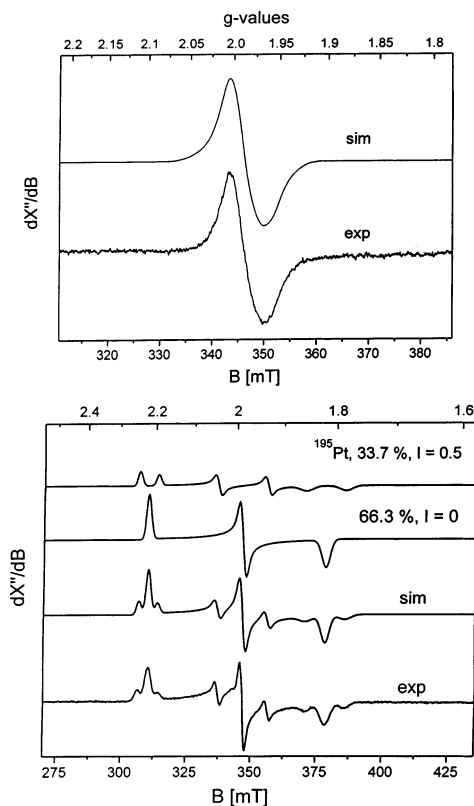
Figure 10. X-band EPR spectra at 30 K of the electrochemically generated monocation (top) and monoanion (bottom) of trans-**6** in frozen CH_3CN solution (0.10 M [TBA]BF$_4$). Conditions: frequency 9.6353 (9.6356) GHz; power 100.6 (50.4) μW; modulation 10.0 (10.0) G. Simulation parameters are given in Table 5.

diamagnetic dication are probably quite similar but we have not been able to deconvolute these data in Table 4.

X-Band EPR Spectra. The monocations and monoanions of complexes **1**−**6** are paramagnetic species with an $S = \frac{1}{2}$ ground state, respectively. Because the report by Holm and Balch in 1966[1] the X-band EPR spectra of $[Ni^{II}(^1L^{ISQ})(^1L^{IBQ})]^+$ and $[Ni^{II}(^1L^{ISQ})(^1L^{PDI})]^-$ have been recorded and discussed rather controversially. As summarized in Table 5, the EPR spectra these monocations and monoanions of square planar species containing two *o*-semiquinonate,[29] two *o*-dithiolate,[30] two *o*-aminothiolate,[26,31] or two *o*-aminophenolate[25] type ligands (in their various oxidized forms) are very similar. The spectra of the monocations display very small *g*-anisotropy, and in some cases, very small hyperfine coupling to the central metal ion (most significantly to Pt^{II}). In contrast, the spectra of the monoanions display a significantly larger *g*-anisotropy irrespective of the nature of the two ligands.

The same observations hold for the EPR spectra of the electrochemically generated monocations and monoanions of complexes **1**−**6**. The results are summarized in Table 5 and Figure 10 exhibits the spectra of [*trans*-**6**]$^+$ and [*trans*-**6**]$^-$ in frozen CH_3CN at 30 K. The spectrum of the monoanion displays $g_z > g_{x,y}$ and large anisotropic hfc's (A(^{195}Pt) = 14, 178, 126 G) indicating that the unpaired electron must possess considerable metal d orbital character. This spectrum is very

(29) Lange, C. W.; Pierpont, C. G. *Inorg. Chim. Acta* **1997**, *263*, 219.
(30) Williams, R.; Billig, E.; Waters, J. H.; Gray, H. B. *J. Am. Chem. Soc.* **1966**, *88*, 43.
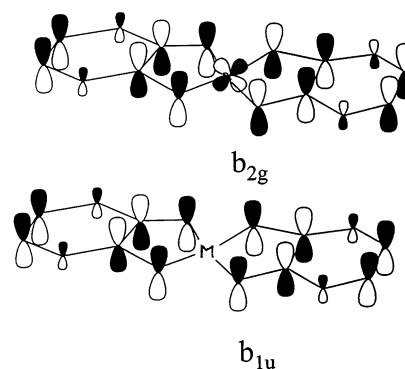(31) Balch, A. L.; Röhrscheid, F.; Holm, R. H. *J. Am. Chem. Soc.* **1965**, *87*, 2301.

Figure 11. Two redox-active MOs of the neutral complexes $[M^{II}(L^{ISQ})_2]$ (M = Ni, Pd, Pt). The b_{1u} MO is lower in energy and the SOMO in the monocations $[M^{II}(L^{ISQ})(L^{IBQ})]^+$ whereas the b_{2g} MO is higher in energy and the SOMO in the monoanions $[M^{II}(L^{ISQ})(L^{PDI})]^-$.
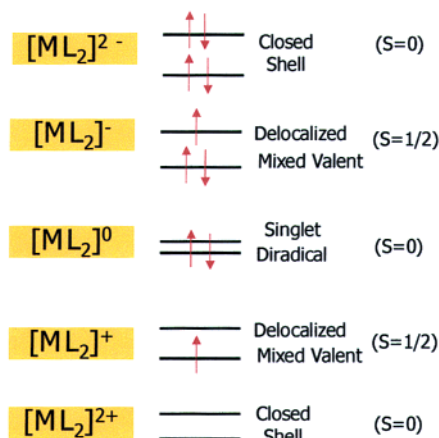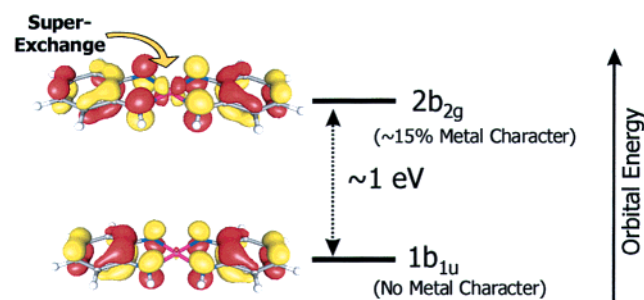

Figure 12. Summary of the electronic structures of the five members of the electron-transfer series $[M^{II}(L)_2]^z$ $z = -2, -1, 0, 1+, 2+$. The two highest energy molecular orbitals b_{1u} and b_{2g} (see also Figure 11) are considered only.

similar to those reported for $[Pt^{II}(L_0^{ISQ})(L_0^{AP}-H)]^-$ and $[Pt^{II}(L_s^{ISQ})(L_s^{AP}-H)]^{-25,26}$ where L_0 represents an *o*-aminophenolate, and L_s the corresponding *o*-aminothiophenolate derivative and $(L^{AP}-H)^{2-}$ is the respective closed shell dianion.

From DFT calculations[19] on $[Pt^{II}(L_0^{ISQ})_2]$, $[Pt^{II}(L_0^{ISQ})(L_0^{AP}-H)]^-$, and $[Pt^{II}(L_0^{ISQ})(L_0^{IBQ})]^+$ we have shown that the magnetic parameters can be understood in terms of a simple model which only involves two molecular orbitals which are depicted in Figures 11 and 12. These are basically the symmetric and antisymmetric combination of the SOMO of the free semiquinonate ligand.

The ground state of the monocation is then $^2B_{1u}$ with the b_{1u} MO in Figure 11 being singly occupied. Because it transforms "ungerade" under inversion it cannot mix with any metal orbital

and, consequently, a large metal hfc cannot be expected. The lack of metal character in the SOMO of the monocations makes the spin−orbit coupling for excited states with the ground state very inefficient. Therefore, there is little angular momentum in the ground-state wave function, and the observed and calculated g-shifts are very small and reflect the organic radical character of the ground state.

For the monoanion a reversed situation is encountered. The orbital b_{2g} transforms "gerade" under inversion and it mixes readily with the out-of-plane d_{xz} orbital of the Pt(II) and acquires thereby some metal character which gives rise to a sizable first-order [195]Pt hyperfine coupling. Because the ground state $^2B_{2g}$ readily mixes with relatively low-lying d−d excited states, it also has a sizable orbital angular momentum that manifests itself in the large g-shifts observed experimentally for the monoanions of **1**−**6**.

It is interesting that acetonitrile solutions of the electrochemically generated monocations of [**1**]$^+$ and [**4**]$^+$ are EPR silent due to complete dimerization of these radical cations in the millimolar concentration range. In contrast, the spectrum of [*trans*-**6**]$^+$ has been observed despite the fact that complex **8**, which represents its diamagnetic dimer, has been isolated. Thus, at the millimolar concentration range of [*trans*-**6**]$^+$ the dimer formation is obviously incomplete.

Discussion

The diamagnetic dianions [M(L^{PDI})$_2$]$^{2-}$ can only be generated at very negative redox potentials, and therefore, we did not attempt their isolation. In addition, these species are very basic indeed and traces of water lead to protonated species. The electronic spectra of such species do not display transitions of significant intensity (>500 M^{-1} cm^{-1}) at wavelengths >350 nm, which is in accord with the presence of two closed-shell dianions (L^{PDI})$^{2-}$ and a divalent metal ion.

Similarly, the spectra of the electrochemically generated, diamagnetic dications [M(L^{IBQ})$_2$]$^{2+}$ indicate the presence of two neutral, closed-shell benzoquinone ligands and a divalent transition metal ion. Attempts to isolate salts containing such dications have failed. It is noteworthy that in the spectra of the dications a fairly intense transition at ∼440 nm with $\epsilon \approx 4 \times 10^3$ M^{-1} cm^{-1} is observed. This has also been reported for [Zn(^{1}L^{IBQ})(OH$_2$)$_2$]$^{2+}$ ($\lambda_{max} = 418$ nm (1.41×10^3 M^{-1} cm^{-1}).[32] Such an absorption maximum has been observed for [**1**]$^{2+}$, [**2**]$^{2+}$, [**3**]$^{2+}$, [**4**]$^{2+}$, [**5**]$^{2+}$, [**6**]$^{2+}$ (Table 4).

Formulation of the above dications and -anions as bis(o-benzoquinone)metal(II) and bis(o-phenylenediamino)metal(II) species has been suggested by Balch and Holm[1] in 1966.

The diamagnetic, neutral complexes [M^{II}(L^{ISQ})$_2$] (**1**−**6**) are best described as singlet diradical complexes containing two o-diiminobenzosemiquinonate(1-) π radicals and a divalent metal ion as suggested by Gray et al.[2] Recent DFT calculations[18] have shown that the singlet−triplet energy gap for [Ni^{II}(^{1}L^{ISQ})$_2$] is of the order of ∼3300 cm^{-1}. Thus, the present crystal structures of **1**, **4**, **5**, and **6** give accurate geometrical details for an N,N-coordinated o-diiminobenzosemi- quinonate(1-) π radical anion (Figure 1). Interestingly, the electronic spectra of species **1**−**6** invariably display a very intense (>4 × 10^4 M^{-1} cm^{-1}) ligand-to-ligand charge-transfer band (LLCT) in the narrow range 715−840 nm. This LLCT-transition is dipole and spin

allowed and is the source of the intense blue-black color of all neutral species. As we show in a forthcoming paper, this transition carries a significant amount of information about the ground-state exchange coupling.

The electronic spectra of the paramagnetic monocations [M(L^{ISQ})(L^{IBQ})]$^+$ $S_t = $ $^1/_2$ (M = Pd, Pt) display an intense ($\epsilon \approx 10^4$ M^{-1} cm^{-1}) intervalence charge-transfer band in the range 1100−1650 nm which allows the assignment as delocalized mixed valence species (class III). As pointed out previously,[19] the singly occupied MO b_{1u} has no metal character, and therefore, the EPR spectra of the monocations display very small g-anisotropy and very small−if any−metal hyperfine coupling. These spectra resemble closely those of organic radicals.[1]

The electronic spectra of the monoanions [M^{II}(L^{ISQ})(L^{PDI})]$^-$ also display an intense ($\epsilon \approx (0.7-2.5) \times 10^4$) intervalence charge-transfer band in the range 900−1350 nm which according to the simple Hush relation $\Delta\bar{\nu}_{1/2} < [2310 \; \bar{\nu}_{max}]^{1/2}$ cm^{-1} allows the classification of these anions as delocalized mixed valence species (class III), where $\Delta\bar{\nu}_{1/2}$ is the full width at half-height, and $\bar{\nu}_{max}$ is the position of the absorption maximum in cm^{-1}.[33] As shown in Figure 12, the SOMO in these anions is the b_{2g} MO which mixes well with d_{xz} metal orbitals and, consequently, sizable metal hyperfine coupling constants and large g-anisotropies are observed.

In the past, the EPR spectrum of the monoanion of [Ni^{II}(2,6-*tert*-butyl-o-benzosemiquinonate)$_2$] (Table 5) has been interpreted[29] as that of a low spin Ni^{III} ion with two closed-shell, O,O-coordinated catecholato ligands [Ni^{III}(cat)$_2$]$^-$. We suggest here that, in fact, a mixed valent species of class III is actually present, namely [Ni^{II}(semiquinonate)(catecholate)]$^-$. For the corresponding anion of the dithiolato analogue [Ni(L$_s^{tBu}$)$_2$] where (L$_s^{tBu}$)$^{2-}$ is the 3,5-di-*tert*-butyl-o-dithiophenolate(2-) anion a similar EPR spectrum has been reported[34] with a rhombic signal ($g_1 = 2.18$, $g_2 = 2.04$, $g_3 = 2.01$) and a hyperfine coupling with a [61]Ni nucleus ($I = $ $^3/_2$) of $A_1 = 13.1$, $A_2 = <1.7$, $A_3 = 5.7$ G. Here, an intense ligand-to-ligand intervalence charge-transfer band at 860 nm has also been reported. Thus, [Ni^{II}(dithionebenzosemiquinonate)(o-dithiophenolate)]$^-$ appears to be the correct formulation for this species.[34]

There are three interesting aspects of the structure of dimeric **7** which merit comment: (i) The two halves of the dication, namely [Ni^{II}(^{2}L^{ISQ})(^{2}L^{IBQ})]$^+$, are held together by a weak direct Ni···Ni interaction at 2.800(1) Å. It is not bridged by any ligands or by hydrogen bonding contacts with water molecules of crystallization or chloride anions. The two Ni atoms are displaced by 0.14 Å from the two planes formed each by four imine nitrogen atoms bound to the Ni ions. They are oriented from one Ni atom toward the other in the dimer indicating a bonding Ni···Ni interaction. (ii) The four N,N-coordinated ligands of the dimer are eclipsed which is indicative of an attractive interaction between the four imine ligands because this configuration maximizes otherwise repulsive nonbonding interactions. (iii) The metrical details of these ligands show that the (^{2}L^{ISQ})$^{1-}$ and (^{2}L^{IBQ})^0 parts have identical C−C and C−N bond lengths which indicates delocalization of the excess electron over both ligands. The C−C and C−N distances observed are the average between the data given in Figure 1 for isolated (^{2}L^{ISQ})$^{1-}$ and (^{2}L^{IBQ})^0 ligands.

(32) Dollberg, C. L.; Turro, C. *Inorg. Chem.* **2001**, *40*, 2484.

(33) Creutz, C. *Progr. Inorg. Chem.* **1983**, *30*, 1.
(34) Sellmann, D.; Binder, H.; Häussinger, D.; Heinemann, F. W.; Sutter, J. *Inorg. Chim. Acta* **2000**, *300*−*302*, 829.

The situation is very similar in **8** and the corresponding two complexes in ref 5 and 22. The Pt···Pt interactions are weak and the two halves of the respective dication adopt an eclipsed conformation and the C−C and C−N bonds are intermediate between those of *N,N*-coordinated $(L^{ISQ})^{1-}$ and $(L^{IBQ})^{0}$ ligands. Thus, a delocalized electronic structure is prevailing in these complexes. There is no evidence for the existence of $[Pt^{III}(L^{ISQ})_2]^+$ halves as indicated in ref 2, 5a, 5b, and 22.

The nature of the metal···metal bond in such formally d^8-d^8 species remains rather unclear although a number of such species have been characterized.[20,21,35] In a recent publication we have shown[23] that the square planar monocations [(bpy)-Pd($^3L^{ISQ}$)]$^+$ dimerize in the solid state through π stacking of two coordinated radical anions (no metal−metal bond). The short distance between the radical planes at 2.923 Å induces an $S = 0$ ground state; it can be viewed as a model for the attractive interaction between ligands in **7** and **8** (and the other two complexes[5,22]) yielding the observed eclipsed configuration. In a subsequent publication we will analyze this metal−metal bond in detail.

Conclusions

The main results of this study are summarized as follows.

For two series of diamagnetic complexes **1−3** and **4−6** containing each two *N,N*-coordinated *o*-diiminobenzosemi-quinonate(1-) π radical anions, $(^{2,3}L^{ISQ})^{1-}$, of the parent ligands 3,5-di-*tert*-butyl-*o*-phenylenediamine and N-phenyl-*o*-phenylene-diamine, $H_2(^2L^{PDI})$ and $H_2(^3L^{PDI})$ and a divalent transition metal ion (Ni, Pd, Pt) the structural and spectroscopic features have been elucidated by X-ray crystallography and UV−vis spectroscopy. The electronic structure of the compounds is best described as singlet diradicals: $[M^{II}(L^{ISQ})_2]$ $S = 0$.

Cyclic voltammetry of **1−6** established that each neutral complex can be reduced successively by two electrons yielding a stable mono- and a less stable dianion. In addition, two successive one-electron oxidations have been observed yielding a mono- and a dication, respectively.

The electronic structure of the diamagnetic dications and dianions are best described as square planar species containing two *o*-diiminobenzoquinones in $[M^{II}(L^{IBQ})_2]^{2+}$ and two *o*-di-iminophenolates(2-) in $[M^{II}(L^{PDI})_2]^{2-}$, respectively.

The interesting monocations and -anions are paramagnetic with an $S = \frac{1}{2}$ ground state, respectively. They are ligand based, delocalized (class III) mixed valent complexes with a divalent d^8 metal ion: $[M^{II}(L^{ISQ})(L^{IBQ})]^+$ and $[M^{II}(L^{ISQ})(L^{PDI})]^-$. EPR and UV−vis spectroscopy of these species show that the cation has a $^2B_{1u}$ ground state whereas the anion possesses a $^2B_{2g}$ ground state. The singly occupied MO b_{1u} of the monocation has no metal character, whereas the SOMO b_{2g} of the anion mixes well with d metal orbitals and, consequently, the EPR signals display sizable metal hyperfine coupling and large *g*-anisotropy.

Finally, we have shown that the monocations dimerize in solution yielding a dication with a significant direct metal···metal interaction (bond). The two halves of the dimers adopt an eclipsed conformation due to ligand···ligand inter-actions at ∼3.0 Å. These dimers possess a diamagnetic ground state.

Supporting Information Available: Figures S1 and S2 displaying cyclic voltammograms of **1**, **3** and **4**, **5**, **6**, respectively; Figure S3 exhibiting the electronic spectra of **1** and **6** and their electrochemically generated monocations and -anions; Figure S4 of **3** and **4** and Figure S5 of **5**; Figure S6 displaying X-band EPR spectra of [**1**]$^-$ and [**4**]$^-$; Figure S7 of [**2**]$^{2+}$, [**2**]$^-$; Figure S8 of [*cis/trans*-**3**]$^+$ and [*cis/trans*-**3**]$^-$; Figure S9 of [**5**]$^+$ and [**5**]$^-$. Complete listings of crystallographic details, atom coordinates, bond lengths and bond angles, thermal displacement parameters, and calculated positional parameters for complexes **1**, **4**, **5**, **6**, **7**, and **8**. This material is available free of charge via the Internet at http://pubs.acs.org.

JA030123U

(35) Chern, S.-S.; Liaw, M.-C.; Peng, S.-M. *J. Chem. Soc., Chem. Commun.* **1993**, 359.